[19]. Histone methylation has a critical role in gene transcription and epigenetic events [27–30].

According to recently published GWAS data [11], two SNPs associated with the risk for CHB in the Korea population were identified. These were the top signals in the genome-wide significance level analysis and were independently associated with *HLA-DP* and *HLA-DQ*, respectively. The authors then confirmed the results in a replication sample, showing that the frequency of their two SNPs strongly associated with CHB; OR = 0.76, 95% CI = 0.68–0.86, $p = 4.51E\text{-}11$ for rs1419881 and OR = 1.26, 95% CI = 1.07–1.47, $p = 2.78E\text{-}06$ for rs652888 [16]. Furthermore, another GWAS study focused on HLA, of hepatitis B vaccinated people in Indonesia, showed that rs652888 was also associated with risk of CHB ($p \leq 0.0001$) in that population [31].

In the present study, however, we found that rs1419881 tended to be associated with chronic HBV infection, based on the results of a comparison between HBV carriers and uninfected subjects. Nonetheless, it did not reach the significance by the Bonferroni corrections, as well as when HBV carriers were compared with patients who had their HBV infection resolved, no association with rs1419881 was observed. The second SNP, rs652888, was not associated with chronic HBV infection in the Thai population. Although our study had sampling error due to small samples, it might be another effect that the result between rs652888 in *EHMT2* gene and chronic hepatitis B in Thai population was not associated. The reason for these negative findings for the two SNPs might be due to the affected gene functions that were not involved with the immune system or processes of persistent infection. Data supporting this notion are to be found in the GWAS data for the Korean population, where pathway analysis of genes involved in the regulation of immune function showed that *TCF19* and *EHMT2* genes are not significantly involved in human immunity [16].

Mapping the position of the two new SNPs showed that rs1419881 located at the 3′ UTR of exon 4, with a tendency towards association with CHB and rs652888 which is not associated with CHB located on an intron. The position of each SNP might affect the phenotype of gene expression and susceptibility to disease, explaining why some are associated with chronic HBV infection, and others not. According to previous publications, the 3′ UTR of the *HLA-DP* region is strongly involved with regulating HLA-DP expression and influences the outcome of HBV infection [32]. In addition, another study showed that variation of the 3′ UTR of HLA-C was strongly associated with HLA-C expression levels and with control of human immunodeficiency virus [33]. This illustrated the general principle that the position of SNPs affects association with diseases.

The prevalence of HBV in Eastern countries, i.e. Asia, sub-Saharan Africa and the Pacific is much higher than in Western Europe and America. Most people in Eastern countries are infected with HBV during childhood and 8–10% of these develop CHB. In contract, the frequency of chronic carriers in Western Europe and North America is ≤1%. Furthermore, previous GWAS and meta-analysis reported that A alleles at rs3077 and rs9277353 have protective effects against CHB. Asian and African populations, especially Chinese, have lower frequencies of A alleles than European and American populations [10,34,35]. Moreover, the previous study showed no associations of rs3077 and rs9277535 with progressive CHB infection; however rs3077 was highly significant associated with HBV infection but not associated with rs9277353 in Caucasian populations [36].

While the frequency of alleles at rs3128917 and rs1419881 in Asian and African populations are quite similar, Northern and Western European populations have high frequencies of the protective T allele at rs3128917 but have low T allele frequencies (a risk allele for CHB) at rs1419881. The allele frequencies of populations in the worldwide for conspicuous details came from dbSNP Short Genetic Variations available at http://www.ncbi.nlm.nih.gov/projects/SNP/snp_ref.cgi. Lastly, both ethnic Eastern and Western populations have similar allele frequencies at rs652888, carrying a risk for CHB, with T allele frequencies very much higher than C allele frequencies, which has a protective effect. In addition, evolution of genomic characteristics, the migratory history of different populations, as well as HBV genotypes [37], HBV carrier rate [38] and pathological procession of liver disease [39] in each country may affect the distribution of *HLA* alleles. This was illustrated by a recent report in two Han Chinese populations (southern and northern) having different distributions of *HLA-DP* genes [39]. Thus, the genetics of the host is one of the factors influencing and predicting disease outcome [40].

According to less number of samples, it might influence statistical power in this study. Thus, we made another statistic meta-analysis of data obtained from previous reports and this study in Table S3. We compared HBV carriers with HBV uninfected subjects, because most previous studies also compared CHB with HBV clearance and/or healthy (negative for any HBV serological markers). Interestingly, all SNPs analyzed by the meta-analysis were significantly associated with HBV carriers. These results could support our data in Thailand. Additionally, no heterogeneity was observed between HBV carriers and HBV-resolved subjects ($P_{het} = 0.10$ for rs3077, 0.79 for rs9277378, and 0.07 for rs3128917), as well as between HBV carriers and HBV uninfected subjects ($P_{het} = 0.10$ for rs3077, 0.02 for rs9277378, 0.91 for rs1419881, and 0.04 for rs652888) except for rs9277378 ($P_{het} = 0.000$), for the minor allele frequency (MAF) of only rs9277378 was different between HapMap-CHB (MAF = 46.3% of G allele) and HapMap-JPT (MAF = 44.8% of T allele).

In the present study, we determined associations of variations at the *HLA-DP* gene with outcome in HBV infected Thai patients and the major homozygous genotypes of rs3077 and rs9277378, but not rs3128917, were significantly associated with HBV carrier status. Although genetic variation of two new SNPs, rs1419881 in the *TCF19* gene and rs652888 in the *EHMT2* gene, were not associated with the outcome of HBV infection in the Thai population, a large-scale study should be required.

Supporting Information

Figure S1 Association of 5 SNPs with HBV carriers, resolved HBV and uninfected subjects in Thailand. The results were compared between percentages of combination of heterozygous genotypes and minor homozygous genotypes (White square) with percentages of major homozygous genotypes (Grey square). Five SNPs applied in this study were rs3077, rs9277378 and rs3128917 in *HLA-DP* gene, rs1419881 in *TCF19* gene and rs652888 in *EHMT2* gene. OR, odds ratio; (lower-upper), 95% confidence interval.
(PPTX)

Table S1 Minor allele frequencies in HCC, CHB, resolved HBV and uninfected subjects in Thailand.
(DOC)

Table S2 The meta-analysis of minor allele frequencies in HBV carriers and resolved HBV.
(DOC)

Table S3 The meta-analysis of minor allele frequencies in HBV carriers and uninfected subject.
(DOC)

Author Contributions

Conceived and designed the experiments: SP TW YP YT. Performed the experiments: NP. Analyzed the data: NP SP SI KM NS. Contributed reagents/materials/analysis tools: PT SO SM. Wrote the paper: NP.

References

1. Kao JH, Chen DS (2002) Global control of hepatitis B virus infection. Lancet Infect Dis 2: 395–403.
2. Zanetti AR, Van Damme P, Shouval D (2008) The global impact of vaccination against hepatitis B: a historical overview. Vaccine 26: 6266–6273.
3. Dandri M, Locarnini S (2012) New insight in the pathobiology of hepatitis B virus infection. Gut 61 Suppl 1: i6–17.
4. Pan CQ, Zhang JX (2005) Natural History and Clinical Consequences of Hepatitis B Virus Infection. Int J Med Sci 2: 36–40.
5. Tran TT, Martin P (2004) Hepatitis B: epidemiology and natural history. Clin Liver Dis 8: 255–266.
6. Pumpens P, Grens E, Nassal M (2002) Molecular epidemiology and immunology of hepatitis B virus infection - an update. Intervirology 45: 218–232.
7. Elgouhari HM, Abu-Rajab Tamimi TI, Carey WD (2008) Hepatitis B virus infection: understanding its epidemiology, course, and diagnosis. Cleve Clin J Med 75: 881–889.
8. Singh R, Kaul R, Kaul A, Khan K (2007) A comparative review of HLA associations with hepatitis B and C viral infections across global populations. World J Gastroenterol 13: 1770–1787.
9. Thio CL, Thomas DL, Karacki P, Gao X, Marti D, et al. (2003) Comprehensive analysis of class I and class II HLA antigens and chronic hepatitis B virus infection. J Virol 77: 12083–12087.
10. Kamatani Y, Wattanapokayakit S, Ochi H, Kawaguchi T, Takahashi A, et al. (2009) A genome-wide association study identifies variants in the HLA-DP locus associated with chronic hepatitis B in Asians. Nat Genet 41: 591–595.
11. Mbarek H, Ochi H, Urabe Y, Kumar V, Kubo M, et al. (2011) A genome-wide association study of chronic hepatitis B identified novel risk locus in a Japanese population. Hum Mol Genet 20: 3884–3892.
12. Wang L, Wu XP, Zhang W, Zhu DH, Wang Y, et al. (2011) Evaluation of genetic susceptibility loci for chronic hepatitis B in Chinese: two independent case-control studies. PLoS One 6: e17608.
13. An P, Winkler C, Guan L, O'Brien SJ, Zeng Z, Consortium HBVS (2011) A common HLA-DPA1 variant is a major determinant of hepatitis B virus clearance in Han Chinese. J Infect Dis 203: 943–947.
14. Nishida N, Sawai H, Matsuura K, Sugiyama M, Ahn SH, et al. (2012) Genome-wide association study confirming association of HLA-DP with protection against chronic hepatitis B and viral clearance in Japanese and Korean. PLoS One 7: e39175.
15. Hu L, Zhai X, Liu J, Chu M, Pan S, et al. (2012) Genetic variants in human leukocyte antigen/DP-DQ influence both hepatitis B virus clearance and hepatocellular carcinoma development. Hepatology 55: 1426–1431.
16. Kim YJ, Young Kim H, Lee JH, Jong Yu S, Yoon JH, et al. (2013) A genome-wide association study identified new variants associated with the risk of chronic hepatitis B. Hum Mol Genet : In press.
17. Ku DH, Chang CD, Koniecki J, Cannizzaro LA, Boghosian-Sell L, et al. (1991) A new growth-regulated complementary DNA with the sequence of a putative trans-activating factor. Cell Growth Differ 2: 179–186.
18. Shinkai Y, Tachibana M (2011) H3K9 methyltransferase G9a and the related molecule GLP. Genes Dev 25: 781–788.
19. Tachibana M, Sugimoto K, Fukushima T, Shinkai Y (2001) Set domain-containing protein, G9a, is a novel lysine-preferring mammalian histone methyltransferase with hyperactivity and specific selectivity to lysines 9 and 27 of histone H3. J Biol Chem 276: 25309–25317.
20. Barrett JC, Fry B, Maller J, Daly MJ (2005) Haploview: analysis and visualization of LD and haplotype maps. Bioinformatics 21: 263–265.
21. Prokunina L, Alarcon-Riquelme ME (2004) Regulatory SNPs in complex diseases: their identification and functional validation. Expert Rev Mol Med 6: 1–15.
22. Yang PL, Althage A, Chung J, Maier H, Wieland S, et al. (2010) Immune effectors required for hepatitis B virus clearance. Proc Natl Acad Sci U S A 107: 798–802.
23. O'Brien TR, Kohaar I, Pfeiffer RM, Maeder D, Yeager M, et al. (2011) Risk alleles for chronic hepatitis B are associated with decreased mRNA expression of HLA-DPA1 and HLA-DPB1 in normal human liver. Genes Immun 12: 428–433.
24. Miller GM, Madras BK (2002) Polymorphisms in the 3′-untranslated region of human and monkey dopamine transporter genes affect reporter gene expression. Mol Psychiatry 7: 44–55.
25. Di Paola R, Frittitta L, Miscio G, Bozzali M, Baratta R, et al. (2002) A variation in 3′ UTR of hPTP1B increases specific gene expression and associates with insulin resistance. Am J Hum Genet 70: 806–812.
26. Ferreira MA, Hottenga JJ, Warrington NM, Medland SE, Willemsen G, et al. (2009) Sequence variants in three loci influence monocyte counts and erythrocyte volume. Am J Hum Genet 85: 745–749.
27. Cho HS, Kelly JD, Hayami S, Toyokawa G, Takawa M, et al. (2011) Enhanced expression of EHMT2 is involved in the proliferation of cancer cells through negative regulation of SIAH1. Neoplasia 13: 676–684.
28. Albert M, Helin K (2010) Histone methyltransferases in cancer. Semin Cell Dev Biol 21: 209–220.
29. Krivtsov AV, Armstrong SA (2007) MLL translocations, histone modifications and leukaemia stem-cell development. Nat Rev Cancer 7: 823–833.
30. Lu Z, Tian Y, Salwen HR, Chlenski A, Godley LA, et al. (2013) Histone-lysine methyltransferase EHMT2 is involved in proliferation, apoptosis, cell invasion, and DNA methylation of human neuroblastoma cells. Anticancer Drugs 24: 484–493.
31. Png E, Thalamuthu A, Ong RT, Snippe H, Boland GJ, el at. (2011) A genome-wide association study of hepatitis B vaccine response in an Indonesian population reveals multiple independent risk variants in the HLA region. Hum Mol Genet 20: 3893–3898.
32. Thomas R, Thio CL, Apps R, Qi Y, Gao X, et al. (2012) A novel variant marking HLA-DP expression levels predicts recovery from hepatitis B virus infection. J Virol 86: 6979–6985.
33. Kulkarni S, Savan R, Qi Y, Gao X, Yuki Y, et al. (2011) Differential microRNA regulation of HLA-C expression and its association with HIV control. Nature 472: 495–498.
34. Guo X, Zhang Y, Li J, Ma J, Wei Z, et al. (2011) Strong influence of human leukocyte antigen (HLA)-DP gene variants on development of persistent chronic hepatitis B virus carriers in the Han Chinese population. Hepatology 53: 422–428.
35. Yan Z, Tan S, Dan Y, Sun X, Deng G, et al. (2012) Relationship between HLA-DP gene polymorphisms and clearance of chronic hepatitis B virus infections: case-control study and meta-analysis. Infect Genet Evol 12: 1222–1228.
36. Vermehren J, Lotsch J, Susser S, Wicker S, Berger A, et al. (2012) A common HLA-DPA1 variant is associated with hepatitis B virus infection but fails to distinguish active from inactive Caucasian carriers. PLoS One 7: e32605.
37. Zeng G, Wang Z, Wen S, Jiang J, Wang L, et al. (2005) Geographic distribution, virologic and clinical characteristics of hepatitis B virus genotypes in China. J Viral Hepat 12: 609–617.
38. Hyams KC (1995) Risks of chronicity following acute hepatitis B virus infection: a review. Clin Infect Dis 20: 992–1000.
39. Li J, Yang D, He Y, Wang M, Wen Z, et al. (2011) Associations of HLA-DP variants with hepatitis B virus infection in southern and northern Han Chinese populations: a multicenter case-control study. PLoS One 6: e24221.
40. Wong DK, Watanabe T, Tanaka Y, Seto WK, Lee CK, et al. (2013) Role of HLA-DP polymorphisms on chronicity and disease activity of hepatitis B infection in Southern Chinese. PLoS One 8: e66920.

JCM
Journals.ASM.org

Application of a Newly Developed High-Sensitivity HBsAg Chemiluminescent Enzyme Immunoassay for Hepatitis B Patients with HBsAg Seroclearance

Noboru Shinkai,[a,b] Kentaro Matsuura,[a,b] Fuminaka Sugauchi,[a,b] Tsunamasa Watanabe,[a] Shuko Murakami,[a] Etsuko Iio,[a,b] Shintaro Ogawa,[a] Shunsuke Nojiri,[b] Takashi Joh,[b] Yasuhito Tanaka[a]

Department of Virology and Liver Unit, Nagoya City University Graduate School of Medical Sciences, Nagoya, Japan[a]; Department of Gastroenterology and Metabolism, Nagoya City University Graduate School of Medical Sciences, Nagoya, Japan[b]

We modified and automated a highly sensitive chemiluminescent enzyme immunoassay (CLEIA) for surface antigen (HBsAg) detection using a combination of monoclonal antibodies, each for a specific epitope of HBsAg, and by improving an earlier conjugation technique. Of 471 hepatitis B virus (HBV) carriers seen in our hospital between 2009 and 2012, 26 were HBsAg seronegative as determined by the Abbott Architect assay. The Lumipulse HBsAg-HQ assay was used to recheck those 26 patients who demonstrated seroclearance by the Abbott Architect assay. The performance of the Lumipulse HBsAg-HQ assay was compared with that of a quantitative HBsAg detection system (Abbott Architect) and the Roche Cobas TaqMan HBV DNA assay (CTM) (lower limit of detection, 2.1 log copies/ml) using blood serum samples from patients who were determined to be HBsAg seronegative by the Abbott Architect assay. Ten patients had spontaneous HBsAg loss. Of 8 patients treated with nucleotide analogues (NAs), two were HBsAg seronegative after stopping lamivudine therapy and 6 were HBsAg seronegative during entecavir therapy. Eight acute hepatitis B (AH) patients became HBsAg seronegative. Of the 26 patients, 16 were HBsAg positive by the Lumipulse HBsAg-HQ assay but negative by the Abbott Architect assay. The differences between the two assays in terms of detectable HBsAg persisted over the long term in the spontaneous loss group (median, 10 months), the NA-treated group (2.5 months), and the AH group (0.5 months). In 9 patients, the Lumipulse HBsAg-HQ assay detected HBsAg when HBV DNA was negative by the CTM assay. HBsAg was also detected by the Lumipulse HBsAg-HQ assay in 4 patients with an anti-HBs concentration of >10 mIU/ml, 3 of whom had no HBsAg escape mutations. The automatic, highly sensitive HBsAg CLEIA Lumipulse HBsAg-HQ is a convenient and precise assay for HBV monitoring.

Today, >400 million people worldwide are hepatitis B virus (HBV) carriers (1). We have monitored HBV markers, such as HBV DNA, hepatitis B surface antigen (HBsAg), hepatitis B e antigen (HBeAg), and HB core-related antigen (HBcrAg), in chronic hepatitis B patients. The measurement of HBV DNA levels by a PCR-based method is the state-of-the-art technique for monitoring HBV replication in clinical practice (2). However, it is suboptimal for chronic hepatitis B patients who are medicated with nucleotide analogues (NAs), as those, in many cases, can decrease HBV DNA to below the limit of detection.

HBsAg is a secreted envelope protein that is continuously shed into the blood as long as HBV infection persists, irrespective of viral replication. Recent advances in HBsAg quantification (qHBsAg) have opened up new perspectives in the study of HBV; qHBsAg levels are correlated with intrahepatic covalently closed circular (ccc) DNA, which is used as a template for viral transcription and maintains the chronic HBV infection state (3–5). Additionally, a correlation between qHBsAg and HBV DNA has been suggested, with the possibility of a role for qHBsAg as a surrogate marker for viral replication put forward, which might identify chronic hepatitis B patients who are likely to be cured with pegylated alpha interferon (6–9).

In Japan, two HBsAg quantification assays are available: the Architect HBsAg-QT (Abbott Japan) (detection range, 50 to 250,000 mIU/ml) and the HISCL HBsAg (Sysmex) (detection range, 30 to 2,500,000 mIU/ml). These two methods have a good correlation and are sensitive over a wide detection range. Recently, Matsubara et al. (10) reported a novel highly sensitive chemiluminescent enzyme immunoassay (CLEIA) that was developed for quantitative HBsAg detection by combining monoclonal antibodies, each specific for a different epitope of the antigen, and employing an improved conjugation technique. It is as sensitive as nucleic acid testing for detecting early HBV infection. We further modified and improved the high-sensitivity assay reagent described above for adaptation to both ferrite microparticles as the solid phase and the automated analyzer system by modification of the optimum combination of monoclonal antibodies. As was recently reported (11), this assay (Lumipulse HBsAg-HQ) had good accuracy, reproducibility, specificity, and sensitivity, and the results correlate well with those of the Abbott Architect. The coefficient of variation in the Lumipulse HBsAg-HQ is <5.9% for samples with a low concentration of HBsAg (11), and the assay was approved by the Japanese government in 2013.

The sensitivity of this assay (5 mIU/ml) was approximately 10-fold higher than that of the Abbott Architect assay (50 mIU/ml). Here, we adapted this assay to monitor chronic hepatitis B

Received 18 March 2013 Returned for modification 29 April 2013
Accepted 6 August 2013
Published ahead of print 14 August 2013
Address correspondence to Yasuhito Tanaka, ytanaka@med.nagoya-cu.ac.jp.

doi:10.1128/JCM.00726-13
The authors have paid a fee to allow immediate free access to this article.

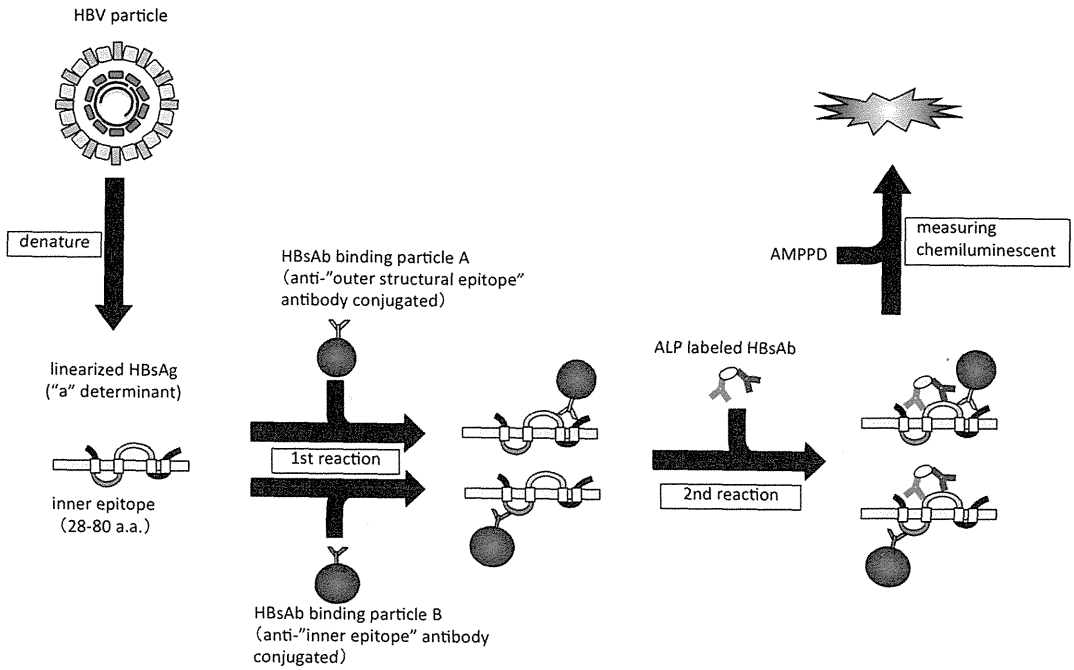

FIG 1 The principle of Lumipulse HBsAg-HQ.

patients with apparent HBsAg seroclearance as determined by the Abbott Architect assay.

MATERIALS AND METHODS

Samples. Four hundred seventy-one patients with chronic HBV infection visited our hospital from 2009 to 2012. One hundred eighty-one patients were asymptomatic carriers, 232 had chronic hepatitis B (CHB), and 58 had liver cirrhosis. Of these, 13 patients took lamivudine, one adefovir, 19 lamivudine plus adefovir, 140 entecavir, 8 entecavir plus adefovir, and 9 tenofovir. Thirty patients with acute HB (AH) infection (8 of whom developed chronic hepatitis) visited our hospital from January 2009 to 2012. We determined HBsAg seroclearance according to the Abbott Architect assay in 26 HBV-infected patients during the observation period. Of these, 10 were not treated with nucleotide analogues (spontaneous HBsAg loss group) and 8 were treated (NA-treated group). Of the 8 NA-treated patients, 2 on lamivudine therapy were HBsAg seronegative after stopping therapy, and the other 6 were HBsAg seronegative during entecavir therapy. Eight AH patients became HBsAg seronegative.

The study protocol conformed to the 1975 Declaration of Helsinki and was approved by the ethics committees of our institutions, and informed consent was obtained from each carrier. We rechecked HBsAg status of the patients by the Lumipulse HBsAg-HQ assay in their serial blood serum samples and compared the results with those of the Architect HBsAg-QT assay.

Methods. (i) Measurement of HBsAg by Lumipulse HBsAg-HQ assay. HBsAg was measured on the two-step sandwich assay principle with a fully automated chemiluminescent enzyme immunoassay system (Lumipulse G1200; Fujirebio, Inc.). The assay principle for this new reagent was based on that previously reported by Matsubara et al. (10). Briefly, samples were pretreated with a solution, including surfactant to disrupt HBV particles, to dissociate HBsAg from HBsAg–anti-HBs complexes and to denature epitopes to a linear form. Linearized HBsAg were then detected using two monoclonal antibodies against external structural regions as determinant "a" and the internal epitope as a capture reagent, with two monoclonal antibodies coupled to alkaline phosphatase as the detector. For the assay procedures, 100 μl blood serum and/or plasma samples together with 20 μl pretreatment solution were incubated with the monoclonal antibodies binding ferrite microparticles at 37°C for 10 min. After automatic washing, 250 μl of the alkaline phosphatase-labeled antibodies were added and further incubated at 37°C for 10 min. After the washing step, 200 μl substrate solution (AMPPD [3-(2′-spiroadamantane)-4-methoxy-4-(3″-phosphoryloxy)phenyl-1,2-dioxetane disodium salt]) (Applied Biosystems, Bedford, MA) was added and incubated at 37°C for 5 min. The relative intensity of chemiluminescence was measured and the HBsAg concentration was calculated by comparison with a standard curve. The range of HBsAg concentrations assayed was 5 to 150,000 mIU/ml, and retesting was accepted with a 200-fold dilution of samples that exceeded this range. In the present study, the cutoff value of HBsAg concentration was set at 5 mIU/ml. HBsAg in blood serum was also quantified at the same intervals using the Abbott Architect HBsAg-QT assay (cutoff value, 50 mIU/ml) (Fig. 1).

(ii) Quantification of HBV DNA. Serum HBV DNA was measured using the TaqMan PCR assay (Cobas TaqMan; Roche Molecular Systems [lower limit of detection, 2.1 log copies/ml]).

(iii) Quantification of HBcrAg. Serum HBcrAg was measured using CLEIA, as described previously (12, 13). Briefly, sodium dodecyl sulfate pretreated serum was incubated with monoclonal antibodies against denatured HBcAg and HBeAg. After washing and incubation with alkaline phosphatase-labeled secondary antibodies, the relative chemiluminescence intensity was measured, and the HBcAg concentration was calculated by comparison with a standard curve generated using a known concentration of recombinant HBeAg-containing peptide. The cutoff value of HBcrAg was 3 log U/ml.

(iv) Quantification of anti-HBs. Serum anti-HBs was measured using the Architect system's anti-HBs. A specimen was considered positive for anti-HBs when the concentration was ≥10.0 mIU/ml.

RESULTS

Table 1 shows clinical data at baseline for the three groups with HBsAg seroclearance according to data from the Abbott Architect assay. In four of 10 spontaneous HBsAg loss cases, HBsAg had already been <50 mIU/ml as measured by the Abbott Architect assay at the first visit. Table 1 shows the characteristics of all 26 patients in these 3 groups. The HBV DNA and HBcrAg levels at

TABLE 1 Clinical data at baseline of 3 groups with HBsAg seroclearance as determined by the Abbott Architect assay

Patient characteristic	Data for group (*n*): Spontaneous HBsAg loss (10)	NA treated (8)[a]	Acute hepatitis (8)
Age at first visit or medication (yr)	60.6 ± 12.6	46.8 ± 12.2	50.5 ± 10.8
Sex (no. of males/no. of females)	10/0	7/1	8/0
Route of infection (no. of vertical/no. of horizontal)	10/0	4/4	0/8
No. with genotype Aa/Ae/Ba/Bj/C	0/0/0/2/8	1/1/1/1/4	1/4/1/0/2
Clinical data			
ALT (median [range]) (IU/liter)	23.5 (8–51)	76 (11–220)	1,682 (455–3,622)
HBeAg (no. positive/no. negative)	0/10	5/3	8/0
HBV DNA (median [range]) (log copies/ml)	2.3 (<2.1 to 3.4)	7.4 (4.1 to >9.1)	6.5 (3.8–8.5)
HBcrAg (median [range]) (log IU/ml)	<3 (<3 to 3.3)	6.8 (4.2–8.6)	7.1 (6.6–8)
Abbott Architect HBsAg-QT detection (median [range]) (mIU/ml)	1,300 (<50 to 10,880)	2,676,800 (9,680–89,679,600)	362,500 (91,200–40,000,000)
NA therapy (no. with none/no. with LVD/no. with ETV)[b]	10/0/0	0/2/6	5/0/3

[a] NA, nucleotide analogue.
[b] LVD, lamivudine; ETV, entecavir.

baseline were significantly higher in the NA-treated and AH groups than in the spontaneous HBsAg loss group. The HBsAg levels at baseline were also significantly higher in the AH group and the NA-treated group than in the spontaneous HBsAg loss group. However, HBsAg became undetectable by the Abbott Architect assay immediately in the AH group (median, 1 month), compared with the NA-treated group (32 months) and the spontaneous HBsAg loss group (78.5 months [excluding 4 patients with HBsAg of ≤50 mIU/ml by the Abbott Architect assay at the first visit]). In 19 of the 26 cases, the HBsAg levels were still detectable by the Lumipulse HBsAg-HQ assay at the time point when they were undetectable by the Abbott Architect assay. At the last time point with detectable HBsAg by Lumipulse HBsAg-HQ assay, the Abbott Architect assay could not detect HBsAg in all 10 spontaneous HBsAg loss patients, but the Abbott Architect assay was also able to detect at the last time point in three (case no. L1, E3, and E5) of eight NA-treated group patients and four (case no. A1, A4, A5, and A7) of eight AH patients. In the spontaneous HBsAg loss group, the decline in HBsAg was slower than in the NA-treated and AH groups (Fig. 2a to 2c). Differences in the median duration between the Abbott Architect and Lumipulse HBsAg-HQ assays were seen at 10 months (excluding 4 patients with HBsAg of <50 mIU/ml by the Abbott Architect assay at the first visit), 2.5 months, and 0.5 months in the spontaneous HBsAg loss group, NA-treated group, and AH group, respectively. We observed the reappearance of HBsAg measured by Lumipulse HBsAg-HQ assay in 2 patients (case no. N4 and N6) in the spontaneous HBsAg loss group, 3 (case no. E1, E3, and E5) in the NA-treated group, and one (case no. A6) in the AH group (Fig. 2a to 2c). At the last time point with detectable HBsAg by the Lumipulse HBsAg-HQ assay, HBV DNA was undetectable by the Cobas TaqMan assay in 4 of 10 spontaneous HBsAg loss patients (40%), 4 of 8 NA-treated patients (50%), and one of 8 AH patients (12.5%). At the last time of detection by the Lumipulse HBsAg-HQ assay, HBcrAg was <3 log U/ml in 8 of 10 spontaneous HBsAg loss patients (80%), 2 of 8 NA-treated patients (25%), and none of the 10 AH patients (0%). At the last time point of detection by the Lumipulse HBsAg-HQ assay, anti-HBs was positive in one of 10 spontaneous HBsAg loss patients (10%), none of the 8 NA-treated patients (0%), and 2 of 10 AH patients (20%) (Tables 2 to 4). In case no. A1 and A7, HBsAg was relatively high at the last time point at which HBsAg was detectable by the Lumipulse HBsAg-HQ assay (Table 4). In case no. A1, however, HBsAg was undetectable by the Abbott Architect and Lumipulse HBsAg-HQ assays after 1 month. In case no. A7, HBsAg was undetectable by the Abbott Architect and Lumipulse HBsAg-HQ assays after 3 months.

To elucidate possible HBs escape mutants, we examined the S gene sequences of all 26 patients at the first visit. Patient N2 had an amino acid G145S mutation, L1 had an amino acid S143T mutation, and L2 had amino acid I126N and F134Y mutations. None had an amino acid G145R mutation. At the last time point that HBsAg was detected by the Abbott Architect assay, anti-HBs was positive in patient N2 (from the spontaneous HBsAg loss group) with an amino acid G145S mutation. We performed an inhibition assay for samples N1 and N2 at the time of Abbott Architect undetectability but Lumipulse HBsAg-HQ detectability to confirm whether the identification of HBsAg by the Lumipulse HBsAg-HQ assay was specific. HBsAg detection of these samples was inhibited, indicating that the Lumipulse HBsAg-HQ assay was indeed specific. The following are three representative cases.

(i) Case no. N7 was a 71-year-old male. His alanine transaminase (ALT) was 19 IU/liter, HBV DNA was 3.7 log copies/ml at his first visit, the HBV genotype was C, HBeAg was negative, and anti-HBe was positive. The HBsAg level as measured by the Abbott Architect assay was 162,000 mIU/ml. The patient was followed as an inactive HB carrier. The last time at which HBsAg was detectable by the Abbott Architect assay was 87 months after the first visit, and it became undetectable in 3 months. However, it was still detectable by the Lumipulse HBsAg-HQ assay (78 mIU/ml). HBV DNA by Cobas TaqMan assay decreased to <2.1 log copies/ml. The Lumipulse HBsAg-HQ assay was still positive even 10 months after the Abbott Architect assay became negative. The HBsAg level measured by the Lumipulse HBsAg-HQ assay was 5.8 mIU/ml at this time (Fig. 3a).

(ii) Case no. E1 was a 51-year-old male who had been infected

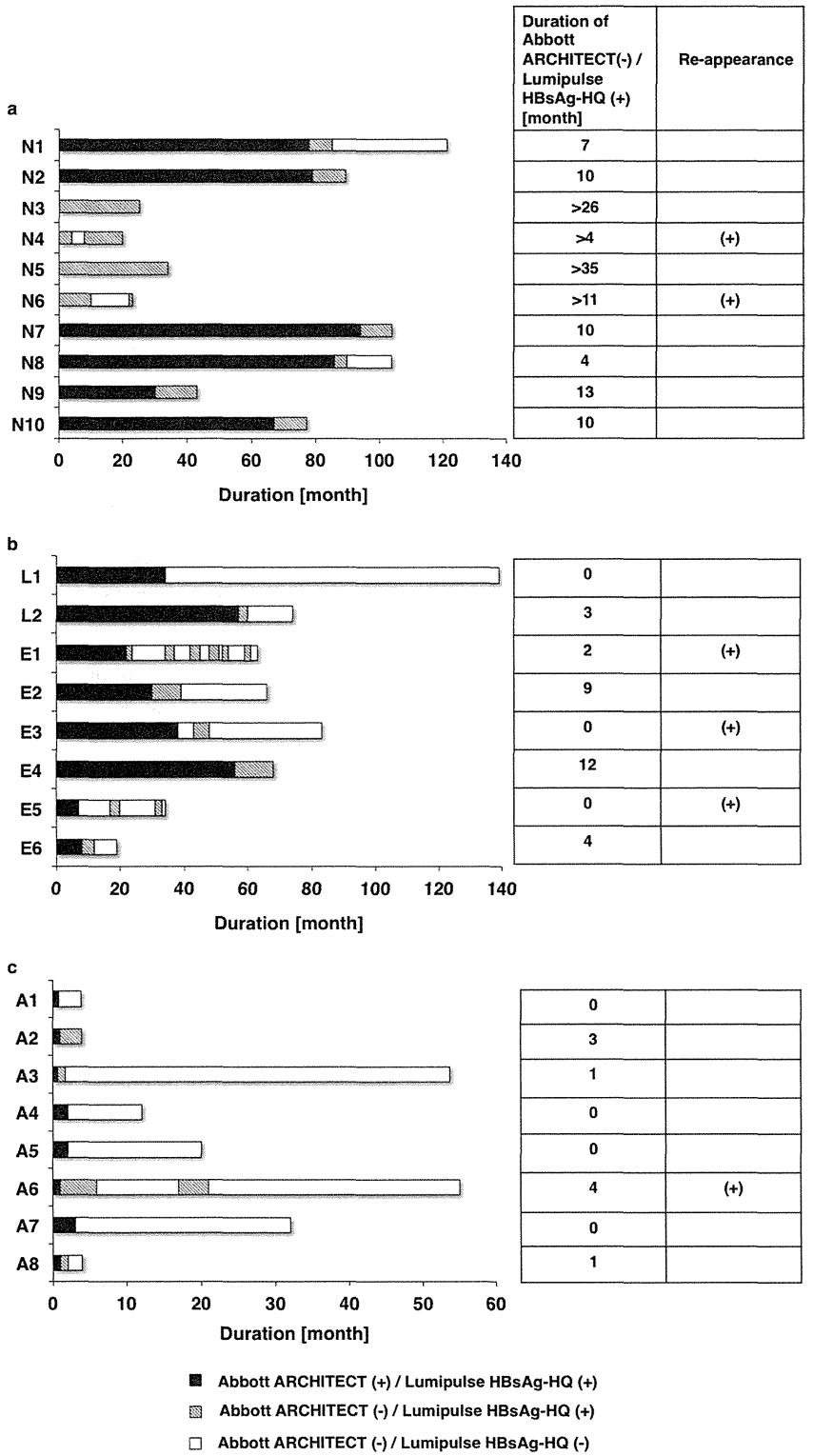

Duration of Abbott ARCHITECT(-) / Lumipulse HBsAg-HQ (+) [month]	Re-appearance
7	
10	
>26	
>4	(+)
>35	
>11	(+)
10	
4	
13	
10	

0	
3	
2	(+)
9	
0	(+)
12	
0	(+)
4	

0	
3	
1	
0	
0	
4	(+)
0	
1	

FIG 2 HBsAg dynamics by the Abbott Architect and Lumipulse HBsAg-HQ assays in the spontaneous HBsAg loss group (a), the NA-treated group (b), and the AH group (c).

with HBV by transfusion in adulthood and had developed chronic hepatitis B. His ALT was 57 IU/liter, HBV DNA was 8.6 copies/ml by the Cobas TaqMan assay, the HBV DNA genotype was Ba, HBeAg was positive, and anti-HBe was negative. The HBsAg level as measured by the Abbott Architect assay was 4,983,730 mIU/ml. The patient was treated with entecavir. After 24 months, HBsAg became undetectable by the Abbott Architect assay, and from this point to the last observation point, the Abbott Architect assay was

TABLE 2 Clinical data of spontaneous HBsAg loss patients at the last time point at which HBsAg was detectable by the Lumipulse HBsAg-HQ assay

Clinical data	Values for patient no.:									
	N1	N2[b]	N3[a,b]	N4[a,b]	N5[a,b]	N6[a,b]	N7[b]	N8	N9[b]	N10[b]
Nucleotide analogue therapy	None	None	None	None	None	None	None	None	None	None
Age (yr)	61	54	91	50	76	63	71	62	62	65
HBeAg (+/−)	−	−	−	−	−	−	−	−	−	−
Abbott Architect HBsAg-QT detection (mIU/ml)	<50	<50	<50	<50	<50	<50	<50	<50	<50	<50
Lumipulse HBsAg-HQ detection (mIU/ml)	8.0	51.0	12.0	8.9	10.4	5	5.8	20.4	11.7	30.3
HBV DNA (log copies/ml)	Not detected	Not detected	<2.1	<2.1	2.9	2.6	<2.1	Not detected	2.7	Not detected
HBcrAg (log IU/ml)	<3	3	<3	<3	3.2	<3	<3	<3	<3	<3
Anti-HBs (mIU/ml)	<10	973.8	<10	<10	<10	<10	<10	<10	<10	<10

[a] Abbott Architect HBsAg-QT assay (IU/ml) was already negative at first visit.
[b] Lumipulse HBsAg-HQ assay was still able to detect HBsAg at the last observation time.

continuously unable to detect HBsAg. The HBsAg level as measured by the Lumipulse HBsAg-HQ assay was 14.7 mIU/ml at the first point that was undetectable by the Abbott Architect assay, and it had been detectable for 3 months. After 3 months, HBsAg became undetectable by the Lumipulse HBsAg-HQ assay and anti-HBs reached >10 mIU/ml. From this point, anti-HBs was continually >10 mIU/ml. Interestingly, after 1 year, HBsAg measured by Lumipulse HBsAg-HQ assay became detectable again (25.2 mIU/ml), although HBV DNA by the Cobas TaqMan and HBsAg by the Abbott Architect assays remained undetectable. At some time points, HBsAg as determined by the Lumipulse HBsAg-HQ assay was detectable, and at the same time, anti-HBs was >10 mIU/ml (Fig. 3b).

(iii) Case no. A6 was a 38-year-old male diagnosed as having acute hepatitis B. After 1 month, HBeAg became seronegative and anti-HBe became seropositive. Three months after the first visit, HBV DNA was <2.1 log copies/ml, HBsAg became undetectable by the Abbott Architect assay, anti-HBs was 22.75 IU/ml, and the Lumipulse HBsAg-HQ assay detected HBsAg. After this time, anti-HBs was continually >10 mIU/ml. Thirteen months after the first visit, the Lumipulse HBsAg-HQ assay detected the reappearance of HBsAg (7.6 mIU/ml), although anti-HBs was still positive at 23.18 IU/ml (Fig. 3c).

DISCUSSION

The Lumipulse HBsAg-HQ assay showed improved sensitivity after disrupting HBV particles, dissociating HBsAg from HBsAg/anti-HBs complexes, and denaturing epitopes into linear forms. A major difference between the Abbott Architect and the Lumipulse HBsAg-HQ assays is that the latter detects HBsAg-anti-HBs complexes as well as small S proteins, which are present 10,000 to 1,000,000 times more frequently than Dane particles. The detection limit of the Lumipulse HBsAg-HQ assay (5 mIU/ml) was 10 times lower than that of the Abbott Architect assay, but there was otherwise a good correlation between the two. In clinical practice, more precise and broader HBsAg dynamics might therefore be followed by using the Lumipulse HBsAg-HQ assay. Differences between the two assays in detectable HBsAg persisted for a long time in the spontaneous HBsAg loss group (median, 10 months), followed by the NA-treated group (2.5 months) and the AH group (0.5 months).

In addition to the significant decrease or loss of all HBV replication in the blood serum, the long-term outcome after HBsAg seroclearance is good if there is no preexisting cirrhosis or viral superinfection. This view is supported by studies showing increased survival, a lower rate of hepatic decompensation, and a reduced frequency of hepatocellular carcinoma (HCC) in patients who have cleared HBsAg (14, 15). In carriers without cirrhosis and with no evidence of viral superinfection (hepatitis C virus [HCV] and/or hepatitis D virus [HDV]) at HBsAg seroclearance, liver function can improve or remain stable and hepatic decompensation rarely occurs; however, the incidence of HCC varies significantly, as was previously reported (16, 17). These discrepancies might depend on concurrent hepatitis, the severity of liver disease, age, and other factors. Yuen et al. (17) reported that HBsAg seroclearance of patients aged ≥50 years was associated with a higher risk of developing HCC than in patients of age <50 years, suggest-

TABLE 3 Clinical data of NA-treated patients at the last time point at which HBsAg was detectable by the Lumipulse HBsAg-HQ assay

Clinical data	Values for patient no.:							
	L1	L2	E1	E2	E3	E4[a]	E5	E6
Nucleotide analogue therapy	LVD	LVD	ETV	ETV	ETV	ETV	ETV	ETV
Age (yr)	62	49	53	40	44	44	67	39
HBeAg (+/−)	−	−	−	−	−	−	−	−
Abbott Architect HBsAg-QT detection (mIU/ml)	80[b]	<50	<50	<50	90[b]	<50	90[b]	<50
Lumipulse HBsAg-HQ detection (mIU/ml)	77.3	5	14.7	8	44.6	6.5	42.5	89
HBV DNA (log copies/ml)	<2.1	Not detected	Not detected	Not detected	3.3	2.2	<2.1	Not detected
HBcrAg (log IU/ml)	<3	3.3	4.3	4.1	3.2	<3	3.8	4.3
Anti-HBs (mIU/ml)	<10	<10	<10	<10	<10	<10	<10	<10

[a] The Lumipulse HBsAg-HQ assay was still able to detect HBsAg at the last observation time.
[b] HBsAg was detectable by both assays at this point, but HBsAg became undetectable at the next point.

TABLE 4 Clinical data of AH patients at the last time point at which HBsAg was detectable by Lumipulse HBsAg-HQassay

Clinical data	Values for patient no.:							
	A1	A2	A3	A4	A5	A6	A7	A8
Nucleotide analogue therapy	None	None	None	None	None	ETV	ETV	ETV
Age (yr)	62	34	53	50	39	39	53	54
HBeAg (+/−)	−	−	−	−	−	−	+	+
Abbott Architect HBsAg-QT detection (mIU/ml)	91,200[a]	<50	<50	240[a]	680[a]	<50	11,500[a]	<50
Lumipulse HBsAg-HQ detection (mIU/ml)	112,289.3	5.6	13.6	180.4	771.9	7.6	12,358.4	34.3
HBV DNA (copies/ml)	3.8	Not detected	2.3	2.2	3	<2.1	<2.1	<2.1
HBcrAg (log IU/ml)	6.8	4.0	5.4	4.9	3.2	3.1	3.7	4.3
Anti-HBs (mIU/ml)	<10	24.41	<10	<10	<10	23.18	<10	<10

[a] HBsAg was detectable by both assays at this point, but HBsAg became undetectable at the next point.

ing that we have to consider the age at which HBsAg becomes undetectable.

In most patients in our study (9 of 10 in the spontaneous HBsAg loss group and 7 of 8 in each of the NA-treated and AH groups), HBV DNA or HBcrAg was still detectable by the Abbott Architect assay at the time of HBsAg seroclearance (data not shown). Suzuki et al. (18) reported that HBcrAg correlates with intrahepatic covalently closed circular DNA in chronic hepatitis B patients. Hence, as the current CLEIA HBsAg quantification methods are inadequate for following some cases of HBV infection, the use of the Lumipulse HBsAg-HQ assay together with HBcrAg and HBV DNA testing might be valuable for evaluating patient response to treatment with interferon and NAs. Additionally, we reported that the measurement of HBcrAg is useful for predicting relapse after the cessation of lamivudine therapy for chronic hepatitis B; an HBcrAg level of <3.4 log U/ml at this time was the only independent predictive factor for the absence of post-treatment relapse (19). Thus, the combination of highly sensitive HBsAg detection by the Lumipulse HBsAg-HQ assay and HBcrAg might improve the accuracy of predicting response to treatment and relapse. Highly sensitive HBsAg detection by the Lumipulse HBsAg-HQ assay might be useful for several clinical applications. First, the Lumipulse HBsAg-HQ assay might replace HBV DNA monitoring by a PCR-based method for blood screening. As shown in Tables 2 to 4, at the last time point that HBsAg was detectable by the Lumipulse HBsAg-HQ assay, HBV DNA was undetectable in 9 of 26 patients (34%) by the Cobas TaqMan assay. This suggests that the sensitivity of the Lumipulse HBsAg-HQ assay for HBV detection was at least as high as that for the Cobas TaqMan assay at some time points. The Lumipulse HBsAg-HQ assay is simpler, more convenient, and less expensive than HBV DNA quantification by real-time PCR. At present in Japan, nucleic acid testing is used for detecting HBV in blood donors, but the Lumipulse HBsAg-HQ assay might substitute for nucleic acid testing for screening HBV if the sensitivity could be improved.

Second, the Lumipulse HBsAg-HQ assay may be useful for detecting occult HBV infection as well as HBV reactivation. Occult HBV infection is defined as infection with detectable HBV DNA but undetectable HBsAg with or without antibodies to HBV core antigen (anti-HBc) and/or anti-HBs (20–22). Recent interest in occult HBV infection has focused on the potential of donors with such infections to transmit the virus to susceptible recipients (23, 24). In this study, we detected HBsAg by the Lumipulse HBsAg-HQ assay in occult hepatitis B virus infection (OBI) patients, including those with HBsAg clearance as determined by the Architect assay (case no. N1, N3, N4, N5, N6, N7, N10, E3, E4, E5, E6, A3, A6, A8, and A9). In case no. N5, even >35 months after HBsAg became undetectable by the Abbott Architect assay, HBsAg was still detectable by the Lumipulse HBsAg-HQ assay. The Lumipulse HBsAg-HQ assay may change the diagnosis of patients defined as having current occult HBV infection. In case no. E1, HBsAg was detectable by the Lumipulse HBsAg-HQ assay at some time points, although HBV DNA by the Cobas TaqMan assay and HBsAg by Abbott Architect assay remained undetectable. In many cases (cases N1, N2, N4, N6, N8, N10, L2, E1, E2, E3, E5, E6, A2, A4, and A6), the HBV DNA and Lumipulse HBsAg-HQ results did not correlate. Interestingly, the original highly sensitive HBsAg assay reported by Matsubara et al. (10) had a similar sensitivity with HBV DNA detection during the acute phase of HBV infection. If the sensitivity of the Lumipulse HBsAg-HQ assay is improved, it would be sensitive enough to monitor HBV reactivation instead of needing to rely on HBV DNA monitoring. More importantly, there have been cases of HBV reactivation in patients with resolved infection (HBsAg-negative, anti-HBc, and/or anti-HBs positive) during the course of chemotherapy and/or immunotherapy (especially therapy with rituximab plus steroids), sometimes proving fatal (25–29). The Lumipulse HBsAg-HQ assay might be more convenient for such screening than TaqMan PCR.

Third, previous CLEIA HBsAg quantification methods, including the Abbott Architect assay, apply monoclonal/polyclonal antibodies against external structural regions within the determinant "a" loop. HBsAg escape mutations, such as G130D, T131N, M133T, and G145R, were found in patients who were positive for anti-HBs but negative for HBsAg (9, 30). Oon et al. (32) reported that HBV carriers, including HCC patients who were negative for HBsAg but positive for anti-HBc and anti-HBs, had the T126S, Q129D, M133L, T140I, and G145R mutations within the S region. Wu et al. (31) reported that amino acid residues at positions 122 and 145 of HBsAg had a major effect on antigenicity and immunogenicity. HBsAg mutants can escape current detection and persist in HBV-infected individuals after the loss of HBsAg (32). In the present study, we therefore determined the HBs amino acid sequences of all cases (with detectable HBV DNA), some of which had amino acid I126N, F134Y, S143T, and G145S (not G145R) mutations. It is possible that these HBsAg mutants escape detection by current HBsAg assays and the sensitivity becomes low (33). Based on the pretreatment, however, the Lumipulse HBsAg-HQ assay was able to detect HBsAg mutants because it uses two monoclonal antibodies against the external structural region as determinant "a" and the internal epitope as the capture target. Additionally, the Lumipulse HBsAg-HQ assay can detect HBsAg from samples with anti-HBs.

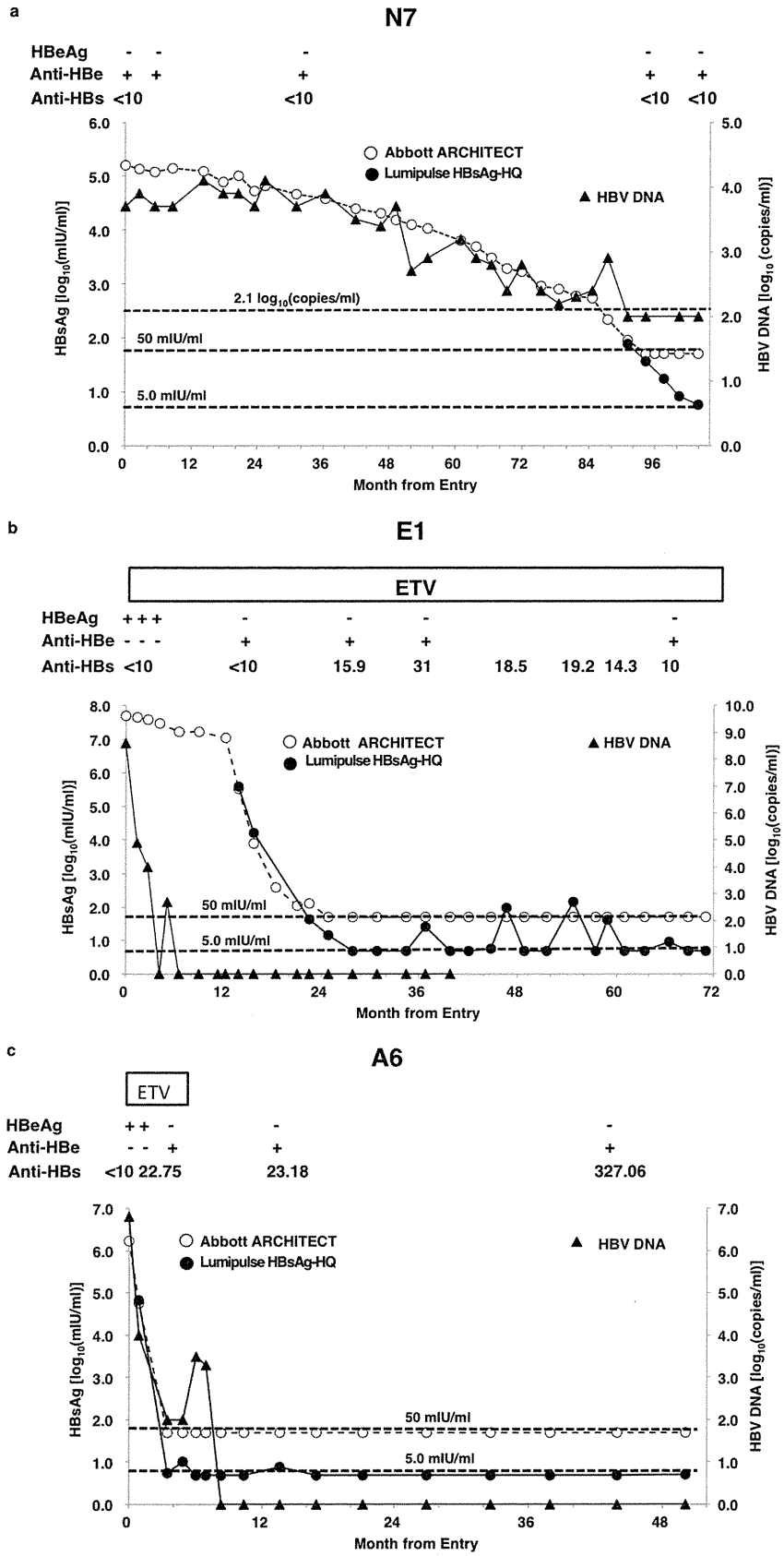

FIG 3 (a) HBsAg and HBV DNA dynamics of case no. N7. The Lumipulse HBsAg-HQ was still positive even 10 months after Abbott Architect results became negative. (b) HBsAg and HBV DNA dynamics of case no. E1. The HBsAg level as measured by the Lumipulse HBsAg-HQ assay was detectable for 3 months after HBsAg became negative by the Abbott Architect assay. After 1 year, HBsAg became detectable by the Lumipulse HBsAg-HQ assay, although HBV DNA was undetectable by the Cobas TaqMan and HBsAg was undetectable by the Abbott Architect assay. At 5 points, HBsAg was detectable by the Lumipulse HBsAg-HQ assay, and the anti-HBs concentration was >10 mIU/ml. (c) HBsAg and HBV DNA dynamics of case no. A6. HBsAg was detectable by the Lumipulse HBsAg-HQ assay for 3 months after HBsAg became negative by the Abbott Architect assay.

In conclusion, the automatic, highly sensitive HBsAg CLEIA Lumipulse HBsAg-HQ assay is a very convenient and precise assay for HBV monitoring in clinical practice.

ACKNOWLEDGMENTS

This study was supported by a grant-in-aid from the Ministry of Education, Culture, Sports, Science, and Technology and a grant-in-aid from the Ministry of Health, Labor, and Welfare of Japan.

The authors declare no conflicts of interest.

REFERENCES

1. **Pan CQ, Zhang JX.** 2005. Natural history and clinical consequences of hepatitis B virus infection. Int. J. Med. Sci. **2**:36–40.
2. **Kohmoto M, Enomoto M, Tamori A, Habu D, Takeda T, Kawada N, Sakaguchi H, Seki S, Shiomi S, Nishiguchi S.** 2005. Quantitative detection of hepatitis B surface antigen by chemiluminescent microparticle immunoassay during lamivudine treatment of chronic hepatitis B virus carriers. J. Med. Virol. **75**:235–239.
3. **Chan HL, Wong VW, Tse AM, Tse CH, Chim AM, Chan HY, Wong GL, Sung JJ.** 2007. Serum hepatitis B surface antigen quantitation can reflect hepatitis B virus in the liver and predict treatment response. Clin. Gastroenterol. Hepatol. **5**:1462–1468.
4. **Werle B, Cinquin K, Marcellin P, Pol S, Maynard M, Trépo C, Zoulim F.** 2004. Evolution of hepatitis B viral load and viral genome sequence during adefovir dipivoxil therapy. J. Viral Hepat. **11**:74–83.
5. **Wursthorn K, Lutgehetmann M, Dandri M, Volz T, Buggisch P, Zollner B, Longerich T, Schirmacher P, Metzler F, Zankel M, Fischer C, Currie G, Brosgart C, Petersen J.** 2006. Peginterferon alpha-2b plus adefovir induce strong cccDNA decline and HBsAg reduction in patients with chronic hepatitis B. Hepatology **44**:675–684.
6. **Brunetto MR, Moriconi F, Bonino F, Lau GK, Farci P, Yurdaydin C, Piratvisuth T, Luo K, Wang Y, Hadziyannis S, Wolf E, McCloud P, Batrla R, Marcellin P.** 2009. Hepatitis B virus surface antigen levels: a guide to sustained response to peginterferon alfa-2a in HBeAg-negative chronic hepatitis B. Hepatology **49**:1141–1150.
7. **Chen CH, Lee CM, Wang JH, Tung HD, Hung CH, Lu SN.** 2004. Correlation of quantitative assay of hepatitis B surface antigen and HBV DNA levels in asymptomatic hepatitis B virus carriers. Eur. J. Gastroenterol. Hepatol. **16**:1213–1218.
8. **Deguchi M, Yamashita N, Kagita M, Asari S, Iwatani Y, Tsuchida T, Iinuma K, Mushahwar IK.** 2004. Quantitation of hepatitis B surface antigen by an automated chemiluminescent microparticle immunoassay. J. Virol. Methods **115**:217–222.
9. **Martinot-Peignoux M, Maylin S, Moucari R, Ripault MP, Boyer N, Cardoso AC, Giuily N, Castelnau C, Pouteau M, Stern C, Aupérin A, Bedossa P, Asselah T, Marcellin P.** 2009. Virological response at 4 weeks to predict outcome of hepatitis C treatment with pegylated interferon and ribavirin. Antivir. Ther. **14**:501–511.
10. **Matsubara N, Kusano O, Sugamata Y, Itoh T, Mizuii M, Tanaka J, Yoshizawa H.** 2009. A novel hepatitis B virus surface antigen immunoassay as sensitive as hepatitis B virus nucleic acid testing in detecting early infection. Transfusion **49**:585–595.
11. **Shinkai N, Tanaka Y, Matsuura K, Kani S, Naganuma H, Mizokami M.** 2010. Evaluation and application of a newly developed highly sensitive HBsAg chemiluminescent enzyme immunoassay for chronic hepatitis B patients. Rinsho Byori **58**:1078–1084. (Article in Japanese.)
12. **Kimura T, Rokuhara A, Sakamoto Y, Yagi S, Tanaka E, Kiyosawa K, Maki N.** 2002. Sensitive enzyme immunoassay for hepatitis B virus core-related antigens and their correlation to virus load. J. Clin. Microbiol. **40**:439–445.
13. **Wong DK, Tanaka Y, Lai CL, Mizokami M, Fung J, Yuen MF.** 2007. Hepatitis B virus core-related antigens as markers for monitoring chronic hepatitis B infection. J. Clin. Microbiol. **45**:3942–3947.
14. **Moucari R, Korevaar A, Lada O, Martinot-Peignoux M, Boyer N, Mackiewicz V, Dauvergne A, Cardoso AC, Asselah T, Nicolas-Chanoine MH, Vidaud M, Valla D, Bedossa P, Marcellin P.** 2009. High rates of HBsAg seroconversion in HBeAg-positive chronic hepatitis B patients responding to interferon: a long-term follow-up study. J. Hepatol. **50**:1084–1092.
15. **van Zonneveld M, Honkoop P, Hansen BE, Niesters HG, Darwish Murad S, de Man RA, Schalm SW, Janssen HL.** 2004. Long-term follow-up of alpha-interferon treatment of patients with chronic hepatitis B. Hepatology **39**:804–810.
16. **Simonetti J, Bulkow L, McMahon BJ, Homan C, Snowball M, Negus S, Williams J, Livingston SE.** 2010. Clearance of hepatitis B surface antigen and risk of hepatocellular carcinoma in a cohort chronically infected with hepatitis B virus. Hepatology **51**:1531–1537.
17. **Yuen MF, Wong DK, Fung J, Ip P, But D, Hung I, Lau K, Yuen JC, Lai CL.** 2008. HBsAg seroclearance in chronic hepatitis B in Asian patients: replicative level and risk of hepatocellular carcinoma. Gastroenterology **135**:1192–1199.
18. **Suzuki F, Miyakoshi H, Kobayashi M, Kumada H.** 2009. Correlation between serum hepatitis B virus core-related antigen and intrahepatic covalently closed circular DNA in chronic hepatitis B patients. J. Med. Virol. **81**:27–33.
19. **Shinkai N, Tanaka Y, Orito E, Ito K, Ohno T, Hirashima N, Hasegawa I, Sugauchi F, Ueda R, Mizokami M.** 2006. Measurement of hepatitis B virus core-related antigen as predicting factor for relapse after cessation of lamivudine therapy for chronic hepatitis B virus infection. Hepatol Res. **36**:272–276.
20. **Hollinger FB.** 2008. Hepatitis B virus infection and transfusion medicine: science and the occult. Transfusion **48**:1001–1026.
21. **Raimondo G, Pollicino T, Cacciola I, Squadrito G.** 2007. Occult hepatitis B virus infection. J. Hepatol. **46**:160–170.
22. **van Hemert FJ, Zaaijer HL, Berkhout B, Lukashov VV.** 2008. Occult hepatitis B infection: an evolutionary scenario. Virol. J. **5**:146. doi:10.1186/1743-422X-5-146.
23. **Dettori S, Candido A, Kondili LA, Chionne P, Taffon S, Genovese D, Iudicone P, Miceli M, Rapicetta M.** 2009. Identification of low HBV-DNA levels by nucleic acid amplification test (NAT) in blood donors. J. Infect. **59**:128–133.
24. **Satake M, Taira R, Yugi H, Hino S, Kanemitsu K, Ikeda H, Tadokoro K.** 2007. Infectivity of blood components with low hepatitis B virus DNA levels identified in a lookback program. Transfusion **47**:1197–1205.
25. **Fukushima N, Mizuta T, Tanaka M, Yokoo M, Ide M, Hisatomi T, Kuwahara N, Tomimasu R, Tsuneyoshi N, Funai N, Sueoka E.** 2009. Retrospective and prospective studies of hepatitis B virus reactivation in malignant lymphoma with occult HBV carrier. Ann. Oncol. **20**:2013–2017.
26. **Law JK, Ho JK, Hoskins PJ, Erb SR, Steinbrecher UP, Yoshida EM.** 2005. Fatal reactivation of hepatitis B post-chemotherapy for lymphoma in a hepatitis B surface antigen-negative, hepatitis B core antibody-positive patient: potential implications for future prophylaxis recommendations. Leuk. Lymphoma **46**:1085–1089.
27. **Pei SN, Chen CH, Lee CM, Wang MC, Ma MC, Hu TH, Kuo CY.** 2010. Reactivation of hepatitis B virus following rituximab-based regimens: a serious complication in both HBsAg-positive and HBsAg-negative patients. Ann. Hematol. **89**:255–262.
28. **Wu JM, Huang YH, Lee PC, Lin HC, Lee SD.** 2009. Fatal reactivation of hepatitis B virus in a patient who was hepatitis B surface antigen negative and core antibody positive before receiving chemotherapy for non-Hodgkin lymphoma. J. Clin. Gastroenterol. **43**:496–498.
29. **Yeo W, Chan TC, Leung NW, Lam WY, Mo FK, Chu MT, Chan HL, Hui EP, Lei KI, Mok TS, Chan PK.** 2009. Hepatitis B virus reactivation in lymphoma patients with prior resolved hepatitis B undergoing anticancer therapy with or without rituximab. J. Clin. Oncol. **27**:605–611.
30. **Chen WN, Oon CJ.** 2000. Hepatitis B virus surface antigen (HBsAg) mutants in Singapore adults and vaccinated children with high anti-hepatitis B virus antibody levels but negative for HBsAg. J. Clin. Microbiol. **38**:2793–2794.
31. **Wu C, Deng W, Deng L, Cao L, Qin B, Li S, Wang Y, Pei R, Yang D, Lu M, Chen X.** 2012. Amino acid substitutions at positions 122 and 145 of hepatitis B virus surface antigen (HBsAg) determine the antigenicity and immunogenicity of HBsAg and influence *in vivo* HBsAg clearance. J. Virol. **86**:4658–4669.
32. **Oon CJ, Chen WN, Goh KT, Mesenas S, Ng HS, Chiang G, Tan C, Koh S, Teng SW, Toh I, Moh MC, Goo KS, Tan K, Leong AL, Tan GS.** 2002. Molecular characterization of hepatitis B virus surface antigen mutants in Singapore patients with hepatocellular carcinoma and hepatitis B virus carriers negative for HBsAg but positive for anti-HBs and anti-HBc. J. Gastroenterol. Hepatol. **17**(Suppl):S491–S496.
33. **Coleman PF.** 2006. Detecting hepatitis B surface antigen mutants. Emerg. Infect. Dis. **12**:198–203.

jbc The Journal of Biological Chemistry

AFFINITY SITES

ASBMB
American Society for Biochemistry and Molecular Biology

Cell Biology:

The Bcl-2 Homology Domain 3 (BH3)-only Proteins Bim and Bid Are Functionally Active and Restrained by Anti-apoptotic Bcl-2 Family Proteins in Healthy Liver

Takahiro Kodama, Hayato Hikita, Tsukasa Kawaguchi, Yoshinobu Saito, Satoshi Tanaka, Minoru Shigekawa, Satoshi Shimizu, Wei Li, Takuya Miyagi, Tatsuya Kanto, Naoki Hiramatsu, Tomohide Tatsumi and Tetsuo Takehara

J. Biol. Chem. 2013, 288:30009-30018.
doi: 10.1074/jbc.M112.443093 originally published online August 28, 2013

THE JOURNAL OF BIOLOGICAL CHEMISTRY VOL. 288, NO. 42, pp. 30009–30018, October 18, 2013

The Bcl-2 Homology Domain 3 (BH3)-only Proteins Bim and Bid Are Functionally Active and Restrained by Anti-apoptotic Bcl-2 Family Proteins in Healthy Liver*[S]

Received for publication, December 7, 2012, and in revised form, August 21, 2013 Published, JBC Papers in Press, August 28, 2013, DOI 10.1074/jbc.M112.443093

Takahiro Kodama, Hayato Hikita, Tsukasa Kawaguchi, Yoshinobu Saito, Satoshi Tanaka, Minoru Shigekawa, Satoshi Shimizu, Wei Li, Takuya Miyagi, Tatsuya Kanto, Naoki Hiramatsu, Tomohide Tatsumi, and Tetsuo Takehara[1]

From the Department of Gastroenterology and Hepatology, Osaka University Graduate School of Medicine, 2-2 Yamada-oka, Suita, Osaka 565-0871, Japan

Background: A fine balance between the anti- and pro-apoptotic multidomain Bcl-2 family proteins controls hepatocyte apoptosis in the healthy liver.
Results: Disruption of the BH3-only proteins Bim and Bid prevents spontaneous hepatocyte apoptosis in the absence of anti-apoptotic Bcl-2 family proteins.
Conclusion: Hepatocyte integrity is maintained by the well orchestrated Bcl-2 network.
Significance: We demonstrated the novel involvement of BH3-only proteins in the healthy Bcl-2 network of the liver.

An intrinsic pathway of apoptosis is regulated by the B-cell lymphoma-2 (Bcl-2) family proteins. We previously reported that a fine rheostatic balance between the anti- and pro-apoptotic multidomain Bcl-2 family proteins controls hepatocyte apoptosis in the healthy liver. The Bcl-2 homology domain 3 (BH3)-only proteins set this rheostatic balance toward apoptosis upon activation in the diseased liver. However, their involvement in healthy Bcl-2 rheostasis remains unknown. In the present study, we focused on two BH3-only proteins, Bim and Bid, and we clarified the Bcl-2 network that governs hepatocyte life and death in the healthy liver. We generated hepatocyte-specific Bcl-xL- or Mcl-1-knock-out mice, with or without disrupting Bim and/or Bid, and we examined hepatocyte apoptosis under physiological conditions. We also examined the effect of both Bid and Bim disruption on the hepatocyte apoptosis caused by the inhibition of Bcl-xL and Mcl-1. Spontaneous hepatocyte apoptosis in Bcl-xL- or Mcl-1-knock-out mice was significantly ameliorated by Bim deletion. The disruption of both Bim and Bid completely prevented hepatocyte apoptosis in Bcl-xL-knock-out mice and weakened massive hepatocyte apoptosis via the additional *in vivo* knockdown of *mcl-1* in these mice. Finally, the hepatocyte apoptosis caused by ABT-737, which is a Bcl-xL/Bcl-2/Bcl-w inhibitor, was completely prevented in Bim/Bid double knock-out mice. The BH3-only proteins Bim and Bid are functionally active but are restrained by the anti-apoptotic Bcl-2 family proteins under physiological conditions. Hepatocyte integrity is maintained by the dynamic and well orchestrated Bcl-2 network in the healthy liver.

Apoptosis via the intrinsic pathway, which is known as the mitochondrial pathway, is regulated by Bcl-2 family members. These members are divided into two groups as follows: core Bcl-2 family proteins, which possess three or four Bcl-2 homology domains (BH1–BH4)[2] and the Bcl-2 homology domain 3 (BH3)-only proteins (1). The former, which are multidomain proteins, are subdivided into pro- and anti-apoptotic proteins. Pro-apoptotic core Bcl-2 family members, such as Bax and Bak, serve as effector molecules of this apoptotic machinery. Upon activation, these members can form pores to permeabilize the mitochondrial outer membrane. Apoptogenic factors, such as cytochrome *c*, can then be released through this membrane into the cytosol, leading to the activation of the caspase cascade and to cellular demise (2). Anti-apoptotic core Bcl-2 family members, including Bcl-2, Bcl-xL, Mcl-1, Bcl-w, and Bfl-1/A1, inhibit the intrinsic pathway of apoptosis by either directly or indirectly antagonizing Bak/Bax activity (3–5). In the original rheostasis model, cellular life and death are regulated by a balance between these anti- and pro-apoptotic core Bcl-2 family proteins (6). We previously reported that the hepatocyte-specific deletion of the *bcl-x* gene resulted in spontaneous hepatocyte apoptosis, and this effect could be completely prevented by the additional deletion of the *bak* and *bax* genes (7). These findings elucidated the importance of the rheostatic balance of the core Bcl-2 family proteins in controlling hepatocyte apoptosis in the healthy liver.

The BH3-only proteins, which include at least eight members, are considered to function as pro-apoptotic sensors, and these proteins set this rheostatic balance toward apoptosis upon activation by a variety of apoptotic stimuli (8, 9). It has been reported that hepatocyte apoptosis through the activation of these BH3-only proteins is involved in the pathophysiology of various liver diseases (10–12). Alternatively, we previously reported that the slight activation of Bid, which can trigger hepatocyte apoptosis, occurs even in the healthy liver and that the inactivation of Bid partially ameliorated spontaneous hepato-

* This work was supported in part by a grant-in-aid for scientific research from the Ministry of Education, Culture, Sports, Science, and Technology of Japan (to T. Takehara).
[S] This article contains supplemental Figs. 1–4.
[1] To whom correspondence should be addressed. Tel.: 81-6-6879-3621; Fax: 81-6-6879-3629; E-mail: takehara@gh.med.osaka-u.ac.jp.

[2] The abbreviations used are: BH1–BH4, Bcl-2 homology domains 1–4; SCID, severe combined immune deficiency; ALT, alanine aminotransferase.

cyte apoptosis in Bcl-xL- or Mcl-1-knock-out mice (7, 13). In the present study, we focused on another BH3-only protein, Bim, which promotes hepatocyte apoptosis upon activation by free fatty acids or by reactive oxygen species in pathological settings, and we further clarified the orchestration of the Bcl-2 network, which governs hepatocyte life and death in the physiological state (10, 11, 14, 15). We found that the disruption of Bim ameliorated hepatocyte apoptosis in Bcl-xL- or Mcl-1-knock-out mice, indicating the involvement of Bim in this hepatocyte apoptosis machinery in the healthy liver as well as that of Bid. Additionally, the deletion of both Bim and Bid prevented the massive hepatocyte apoptosis caused by the inhibition of both Bcl-xL and Mcl-1, suggesting that Bim and Bid are functionally active in the healthy liver and are essential regulators for promoting the intrinsic pathway of apoptosis in hepatocytes in the absence of anti-apoptotic Bcl-2 family proteins. Our present study unveiled the fine and dynamic Bcl-2 networks, the orchestration of which determines hepatocyte life and death in the healthy liver.

EXPERIMENTAL PROCEDURES

Mice—Mice carrying a *bcl-x* gene with two *loxP* sequences at the promoter region and a second intron (*bcl-x*$^{flox/flox}$), mice carrying an *mcl-1* gene encoding amino acids 1–179 flanked by two *lox*P sequences, and heterozygous *alb-cre* transgenic mice expressing the Cre recombinase gene under regulation of the *albumin* gene promoter have been described previously (16–18). Hepatocyte-specific Bcl-xL-knock-out mice (*bcl-x*$^{flox/flox}$*alb-cre*) (17), hepatocyte-specific Mcl-1-knock-out mice (*bcl-x*$^{flox/flox}$*alb-cre*) (13), systemic Bid-knock-out mice (*bid*$^{-/-}$) (12), and Bcl-xL/Bid double knock-out mice (*bid*$^{-/-}$*bcl-x*$^{flox/flox}$*alb-cre*) (7) have also been described previously. We purchased C57BL/6J mice from Charles River (Osaka, Japan), systemic Bim-knock-out mice (*bim*$^{-/-}$) from the Jackson Laboratory (Bar Harbor, ME), and NOD/ShiJic-*scid* Jcl mice from Clea Japan Inc. (Osaka, Japan). We generated Bcl-xL/Bim double knock-out mice (*bim*$^{-/-}$*bcl-x*$^{flox/flox}$*alb-cre*), Mcl-1/Bim double knock-out mice (*bim*$^{-/-}$*mcl-1*$^{flox/flox}$*alb-cre*), Bcl-xL/Bim/Bid triple knock-out mice (*bim*$^{-/-}$*bid*$^{-/-}$*bcl-x*$^{flox/flox}$*alb-cre*), and Bim/Bid double knock-out mice (*bim*$^{-/-}$*bid*$^{-/-}$) by mating the strains. We generated mice with a hepatocyte-specific deletion of Mcl-1 and homozygote severe combined immune deficiency (SCID) mutations (*mcl-1*$^{flox/flox}$*prkdc*$^{scid/scid}$*alb-cre*) by mating hepatocyte-specific Mcl-1-knock-out mice (*bcl-x*$^{flox/flox}$*alb-cre*) and NOD/ShiJic-*scid* Jcl mice. Genotyping of *prkdc*^{scid} gene mutation was performed by the PCR-confronting two-pair primer (PCR-CTPP) method reported previously (19). The mice were maintained in a specific pathogen-free facility and were afforded humane care under approval from the Animal Care and Use Committee of Osaka University Medical School.

Histological Analyses—Liver sections were stained with hematoxylin and eosin (H&E). To detect apoptotic cells, the liver sections were also subjected to staining by terminal deoxynucleotidyltransferase-mediated deoxyuridine triphosphate nick-end labeling (TUNEL) according to a procedure reported previously (20). For immunohistochemical detection of cleaved caspase-3, the liver sections were incubated with the polyclonal rabbit anti-cleaved caspase-3 antibody (Cell Signaling Technology, Beverly, MA) according to a procedure reported previously (20).

Caspase-3/7 Activity—Serum caspase-3/7 activity was measured by a luminescent substrate assay for caspase-3 and caspase-7 (Caspase-Glo assay, Promega) according to the manufacturer's protocol.

Western Blot Analysis—Liver tissue was lysed in lysis buffer (1% Nonidet P-40, 0.5% sodium deoxycholate, 0.1% SDS, 1× protein inhibitor mixture (Nacalai tesque, Kyoto, Japan), 1× phosphatase inhibitor mixture (Nacalai tesque), and phosphate-buffered saline, pH 7.4). The liver lysates were cleared by centrifugation at 10,000 × *g* for 15 min at 4 °C. The protein concentrations were determined using a bicinchoninic acid protein assay kit (Pierce). The protein lysates were electrophoretically separated with SDS-polyacrylamide gels and were transferred onto a polyvinylidene fluoride membrane. For immunodetection, the following antibodies were used: a rabbit polyclonal antibody to Bcl-xL (Santa Cruz Biotechnology, Inc.), a rabbit polyclonal antibody to Bid, a rabbit polyclonal antibody to Bax, a rabbit polyclonal antibody to cleaved caspase-3, a rabbit polyclonal antibody to cleaved caspase-7, a rabbit polyclonal antibody to Puma (Cell Signaling Technology, Beverly, MA), a rabbit monoclonal antibody to Bad, a rabbit polyclonal antibody to Noxa (Abcam, Cambridge, MA), a rabbit polyclonal antibody to Bak (Millipore, Billerica, MA), a rabbit polyclonal antibody to Bim (Enzo Life Sciences Inc., Farmingdale, NY), a rabbit polyclonal antibody to Mcl-1 (Rockland, Gilbertsville, PA), and a mouse monoclonal antibody to β-actin (Sigma-Aldrich).

Real-time Reverse Transcription Polymerase Chain Reaction (Real-time RT-PCR) for mRNA—Total RNA was extracted from liver tissues using an RNeasy minikit (Qiagen, Valencia, CA), was reverse-transcribed, and was subjected to real-time RT-PCR as described previously (21). The mRNA expression of specific genes was quantified using TaqMan gene expression assays (Applied Biosystems, Foster City, CA) as follows: murine *bcl2l11* (assay ID: Mm00437796_m1), murine *fas* (assay ID: Mm01204974_m1), murine *bik* (assay ID: Mm00476123_m1), murine *hrk* (assay ID: Mm01208086_m1), murine *bmf* (assay ID: Mm00506773_m1), and murine *actb* (assay ID: Mm02619580_g1 or Mm00607939_s). The transcript levels are presented as -fold inductions.

siRNA-mediated in Vivo Knockdown—The hepatocyte-specific Bcl-xL-knock-out mice (*bcl-x*$^{flox/flox}$*alb-cre*) and the Bcl-xL/Bim/Bid triple knock-out mice (*bim*$^{-/-}$*bid*$^{-/-}$*bcl-x*$^{flox/flox}$*alb-cre*) were injected with 5 mg/kg *in vivo* grade siRNA against *mcl-1* (MSS275671_e0N), which was mixed with Invivofectamine (Invitrogen), via the tail vein according to the manufacturer's protocol. The mice were sacrificed and examined as indicated by the time courses. The Stealth RNAi negative control with low GC content (Invitrogen) was used as the control.

In Vivo ABT-737 Experiment—ABT-737 was dissolved in a mixture of 30% propylene glycol, 5% Tween 80, and 65% D5W (5% dextrose in water) with pH 4–5. ABT-737 (100 mg/kg) was intraperitoneally administered to the Bim/Bid double knock-

out mice ($bim^{-/-}bid^{-/-}$) or to the Bid-knock-out mice ($bid^{-/-}$). The mice were sacrificed and examined 6 h later.

Statistical Analysis—All of the data are expressed as means ± S.D. unless otherwise indicated. Statistical analyses were performed using an unpaired Student's *t* test or a one-way analysis of variance unless otherwise indicated. When the analyses of variance were applied, the differences in the mean values among the groups were examined by Scheffe's post hoc correction unless otherwise indicated. $p < 0.05$ was considered statistically significant.

RESULTS

The Disruption of Bim Alleviated Spontaneous Hepatocyte Apoptosis in Hepatocyte-specific Bcl-xL-knock-out Mice—To investigate the involvement of the BH3-only protein Bim in the hepatocyte apoptosis caused by Bcl-xL deficiency, hepatocyte-specific Bcl-xL-knock-out mice ($bcl\text{-}x^{fl/fl}alb\text{-}cre$) were mated with systemic Bim-knock-out mice ($bim^{-/-}$). Offspring from the mating of $bim^{+/-}bcl\text{-}x^{fl/fl}alb\text{-}cre$ mice and $bim^{+/-}bcl\text{-}x^{fl/fl}$ mice were examined at 6 weeks of age. A Western blot study confirmed the disappearance of both Bcl-xL and Bim protein expression in the liver tissue of the double knock-out mice ($bim^{-/-}bcl\text{-}x^{fl/fl}alb\text{-}cre$) (Fig. 1*A*). In agreement with our previous report (7, 17), H&E staining of the liver sections showed an increase in the number of hepatocytes, with chromatin condensation and cytosolic shrinkage in the liver lobules of the Bcl-xL-knock-out mice (Fig. 1*B*). The staining also showed a significant increase in TUNEL-positive cells and cleaved caspase-3-positive cells in the liver (Fig. 1, *B–D*). Consistent with these histological observations, the levels of serum caspase-3/7 activity and serum alanine aminotransferase (ALT), which can be used as indicators of hepatocyte apoptosis (22, 23), were significantly higher in the Bcl-xL-knock-out mice than in their wild-type littermates (Fig. 1, *E* and *F*). Additionally, cleaved caspse-3 and -7 were detected in the livers of the Bcl-xL-knock-out mice by Western blotting (Fig. 1*A*). All of these findings indicated spontaneous hepatocyte apoptosis in these mice. Bim-knock-out mice did not show any phenotypes in the liver under physiological conditions (Fig. 1, *B–F*). Alternatively, the disruption of Bim significantly improved all of the parameters that are indicative of hepatocyte apoptosis in Bcl-xL-knock-out mice, including the TUNEL-positive cell counts, cleaved caspase-3-positive cell counts, serum ALT levels, and serum caspase-3/7 activity (Fig. 1, *B–F*). These findings clearly demonstrated that Bim was involved in the hepatocyte apoptosis caused by Bcl-xL disruption. It should be noted that the gene and protein expression levels of Bim were not different between the Bcl-xL-knock-out mice and their wild-type littermates (Fig. 1, *A* and *G*), indicating that the Bim expression levels observed in the healthy liver could induce hepatocyte apoptosis in the absence of the Bcl-2 family proteins.

The Disruption of Bim Alleviated Spontaneous Hepatocyte Apoptosis in Hepatocyte-specific Mcl-1-knock-out Mice—Of the five members of the anti-apoptotic Bcl-2 family proteins, we previously reported that Mcl-1 and Bcl-xL played a pivotal anti-apoptotic role in maintaining hepatocyte integrity in the healthy liver (13). We thus examined the role of Bim in the hepatocyte apoptosis caused by Mcl-1 deficiency. We generated Mcl-1/Bim double knock-out mice ($bim^{-/-}mcl\text{-}1^{fl/fl}alb\text{-}cre$) by mating the hepatocyte-specific Mcl-1-knock-out mice ($mcl\text{-}1^{fl/fl}alb\text{-}cre$) with the systemic Bim-knock-out mice ($bim^{-/-}$). A Western blot study confirmed the disappearance of both Mcl-1 and Bim protein expression in the liver tissue of the double knock-out mice ($bim^{-/-}mcl\text{-}1^{fl/fl}alb\text{-}cre$) (Fig. 2*A*). Consistent with our previous report (13), hepatocyte-specific Mcl-1-knock-out mice showed apoptosis phenotypes very similar to those of the Bcl-xL-knock-out mice, as assessed by TUNEL staining (Fig. 2, *B* and *C*), cleaved caspase-3 staining (Fig. 2, *B* and *D*), serum caspase-3/7 activity (Fig. 2*E*), and serum ALT levels (Fig. 2*F*). In contrast, Mcl-1/Bim double knock-out mice showed significant improvement in these parameters (Fig. 2, *B–F*), indicating that Bim is also involved in the hepatocyte apoptosis induced by the disruption of Mcl-1.

The Disruption of Bim and Bid Prevented Spontaneous Hepatocyte Apoptosis in Hepatocyte-specific Bcl-xL-knock-out Mice—We previously reported that a small amount of Bid, which is another BH3-only protein, was constitutively active and was involved in the spontaneous hepatocyte apoptosis in Bcl-xL- or Mcl-1-knock-out mice (7, 13). We thus examined whether these BH3-only proteins redundantly or cooperatively promoted hepatocyte apoptosis in the absence of Bcl-xL. To this end, Bim/Bid/Bcl-xL triple knock-out mice ($bim^{-/-}bid^{-/-}bcl\text{-}x^{fl/fl}alb\text{-}cre$) were generated by mating the Bim/Bcl-xL double knock-out mice ($bim^{-/-}bcl\text{-}x^{fl/fl}alb\text{-}cre$) with the Bid/Bcl-xL double knock-out mice ($bid^{-/-}bcl\text{-}x^{fl/fl}alb\text{-}cre$). The offspring from the mating of $bim^{+/-}bid{-/-}bcl\text{-}x^{fl/fl}alb\text{-}cre$ mice with $bim^{+/-}bid^{-/-}bcl\text{-}x^{fl/fl}$ mice were examined at 6 weeks of age. A Western blot study confirmed that Bcl-xL, Bid, and Bim protein expression disappeared from the liver tissue of the triple knock-out mice ($bim^{-/-}bid^{-/-}bcl\text{-}x^{fl/fl}alb\text{-}cre$) (Fig. 3*A*). Liver sections of the Bim/Bid/Bcl-xL triple knock-out mice were histologically normal compared with those of the Bid/Bcl-xL double knock-out mice ($bim^{+/+}bid^{-/-}bcl\text{-}x^{fl/fl}alb\text{-}cre$), which still contained some hepatocytes with apoptotic morphologies (Fig. 3*B*). Both the number of TUNEL-positive cells and the serum caspase-3/7 activity in the triple knock-out mice were significantly lower than those in the Bid/Bcl-xL double knock-out mice and did not differ from their control Bid-knock-out or Bim/Bid double knock-out littermates (Fig. 3, *B–D*). Moreover, in contrast to the mild elevation of serum ALT levels in the Bid/Bcl-xL double knock-out mice, the levels in the triple knock-out mice were completely normal (Fig. 3*E*). These findings demonstrated that hepatocyte apoptosis in the absence of Bcl-xL was completely dependent on these two BH3-only proteins.

Bim and Bid Are Essential Regulators for the Promotion of the Intrinsic Pathway of Apoptosis in Hepatocytes in the Absence of Anti-apoptotic Bcl-2 Family Proteins—We then attempted to further examine the involvement of Bim and Bid in hepatocyte apoptosis in the absence of both Bcl-xL and Mcl-1, which are two major anti-apoptotic proteins in the liver. Because, as we reported (13), the hepatocyte-specific Bcl-xL and Mcl-1 double knock-out mice died within 1 day after birth due to impaired liver development, we performed an siRNA-mediated *in vivo* knockdown of *mcl-1* in the Bcl-xL-knock-out mice and in the Bim/Bid/Bcl-xL triple knock-out mice. *mcl-1* siRNA administration efficiently reduced Mcl-1 protein expression in the liver

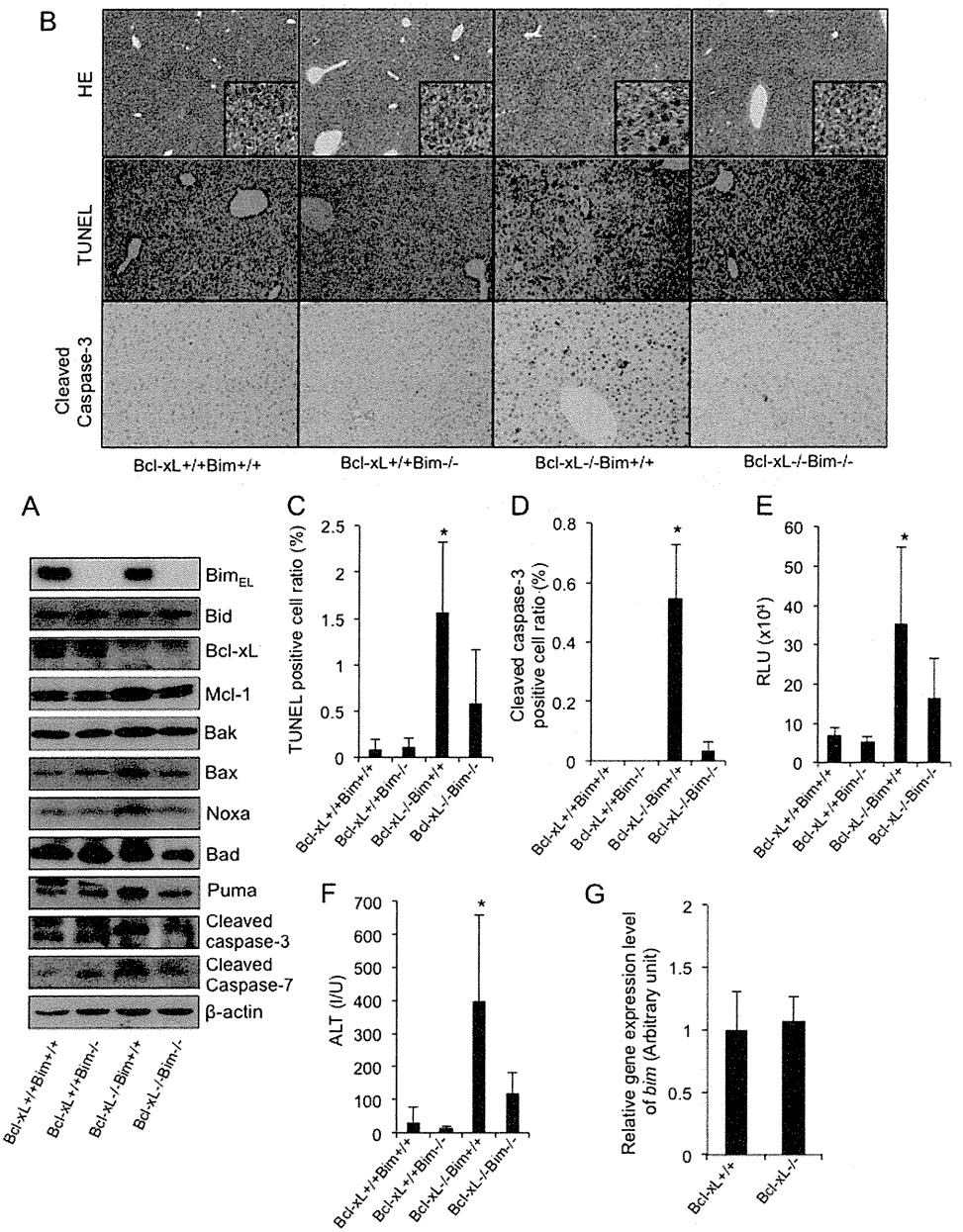

FIGURE 1. **The disruption of Bim alleviated spontaneous hepatocyte apoptosis in the absence of Bcl-xL.** *A–F*, the offspring from the mating of *bim*±*bcl-x*$^{flox/flox}$*alb-cre* mice with *bim*±*bcl-x*$^{flox/flox}$ mice were examined at 6 weeks of age. *Bcl-xL*$^{+/+}$ and *Bcl-xL*$^{-/-}$, *bcl-x*$^{flox/flox}$ and *bcl-x*$^{flox/flox}$*alb-cre*, respectively. *A*, Western blot analysis of whole liver lysates for the expression of Bim$_{EL}$, Bid, Bcl-xL, Mcl-1, Bak, Bax, Noxa, Bad, Puma, cleaved caspase-3, cleaved caspase-7, and β-actin. *B*, representative images for liver histology stained with hematoxylin-eosin (*HE*), TUNEL, and cleaved caspase-3 (original magnifications, ×100 (*large panels*) and ×400 (*insets*)); *black arrows* indicate apoptotic bodies. *C*, TUNEL-positive cell ratio; $n = 8$ mice/group; *, $p < 0.05$ *versus* all. *D*, cleaved caspase-3-positive cell ratio; $n = 3$ mice/group; *, $p < 0.05$ *versus* all. *E*, serum caspase-3/7 activity; $n = 11$ mice/group; *, $p < 0.05$ *versus* all. *F*, serum ALT levels; $n = 13$ mice/group; *, $p < 0.05$ *versus* all. *G*, offspring from the mating of *bcl-x*$^{flox/flox}$*alb-cre* mice with *bcl-x*$^{flox/flox}$ mice were examined at 6 weeks of age. *Bcl-xL*$^{+/+}$ and *Bcl-xL*$^{-/-}$, *bcl-x*$^{flox/flox}$ and *bcl-x*$^{flox/flox}$*alb-cre*, respectively. *bim* mRNA levels in the whole liver tissue were determined by real-time RT-PCR; $n = 6$ mice/group. *Error bars*, S.D. *RLU*, relative light units; *I/U*, international units.

tissue of both mice (Fig. 4*A*), but it caused severe liver injury only in the Bcl-xL-knock-out mice (Fig. 4*B*) when assessed by the H&E staining of liver sections. Notably, *mcl-1* siRNA administration caused massive hepatocyte apoptosis in the Bcl-xL-knock-out mice, but this apoptosis was weakened in the Bim/Bid/Bcl-xL triple knock-out mice, as evidenced by the TUNEL staining of the liver sections, serum caspase-3/7 activity, and serum ALT levels (Fig. 4, *C–E*). In agreement with these findings, *mcl-1* siRNA treatment impaired the liver function of the Bcl-xL-knock-out mice, as evidenced by an increase in the serum bilirubin levels, but not the liver function of the triple knock-out mice (Fig. 4*F*). These findings demonstrated that the massive hepatocyte apoptosis and liver failure caused by decreases in these anti-apoptotic Bcl-2 family proteins were dependent on Bid and Bim.

The Presence of Bim- and Bid-induced Constant BH3 Stress in the Healthy Liver Causes Hepatotoxicity with the Use of Anti-cancer Agents That Target the Anti-apoptotic Bcl-2 Family Proteins—Recent advances in cancer therapy have enabled the selective targeting of some anti-apoptotic Bcl-2 family proteins,

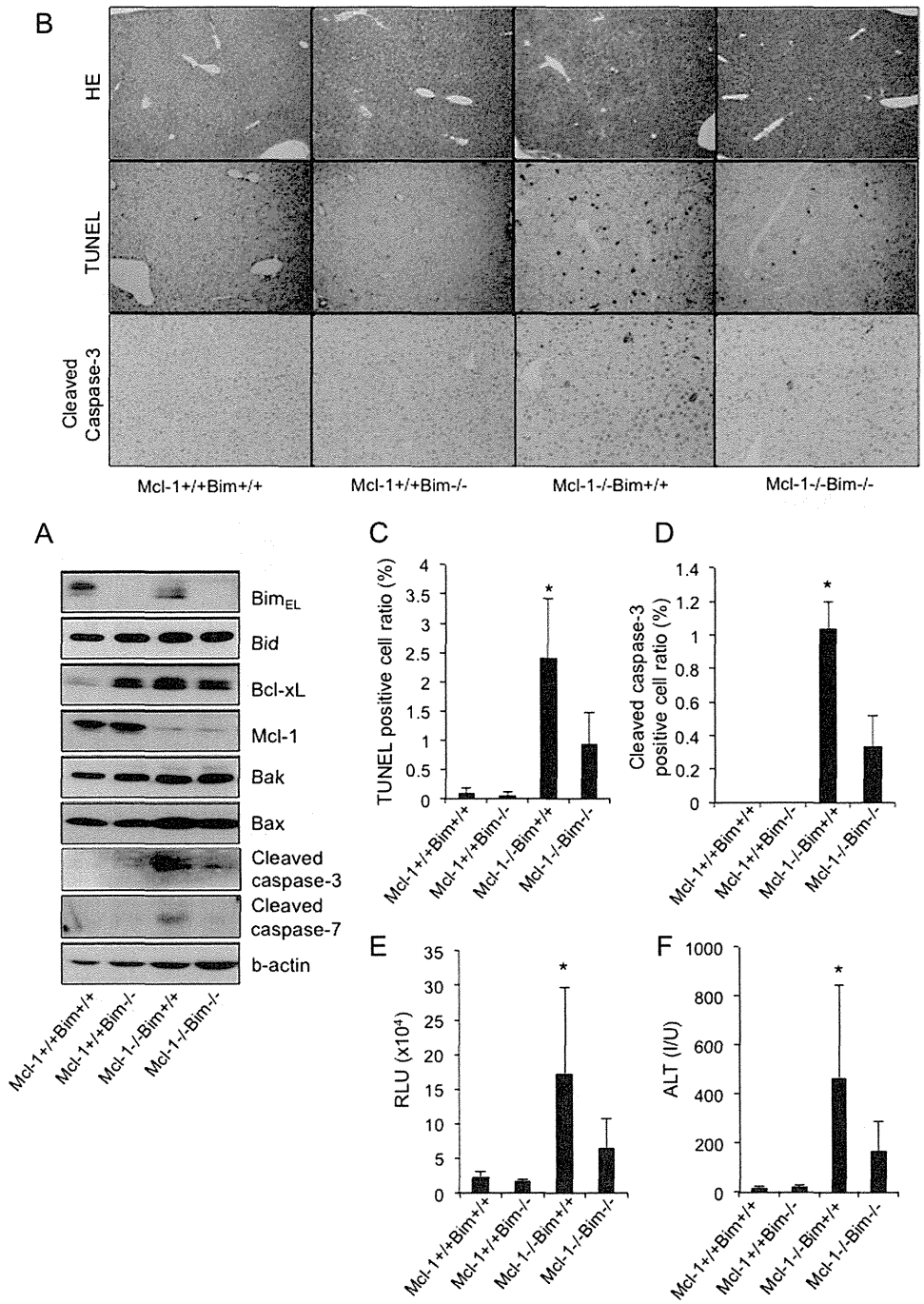

FIGURE 2. **The disruption of Bim alleviated spontaneous hepatocyte apoptosis in the absence of Mcl-1.** The offspring from the mating of *bim*$^{+-}$*mcl-1*$^{flox/flox}$*alb-cre* mice with *bim*$^{+/-}$*mcl-1*$^{flox/flox}$ mice were examined at 6 weeks of age. *Mcl-1*$^{+/+}$ and *Mcl-1*$^{-/-}$, *mcl-1*$^{flox/flox}$ and *mcl-1*$^{flox/flox}$*alb-cre*, respectively. *A*, Western blot analysis of whole liver lysates for the expression of Bim$_{EL}$, Bid, Bcl-xL, Mcl-1, Bak, Bax, cleaved caspase-3, cleaved caspse-7, and β-actin. *B*, representative images for liver histology stained with hematoxylin-eosin (*HE*), TUNEL, and cleaved caspase-3 (original magnification, ×100). *C*, TUNEL-positive cell ratio; $n = 3$–6 mice/group; *, $p < 0.05$ *versus* all. *D*, cleaved caspase-3-positive cell ratio; $n = 3$ mice/group; *, $p < 0.05$ *versus* all. *E*, serum caspase-3/7 activity; $n = 9$–15 mice/group; *, $p < 0.05$ *versus* all. *F*, serum ALT levels; $n = 9$–15 mice/group; *, $p < 0.05$ *versus* all. *Error bars*, S.D. *RLU*, relative light units; *I/U*, international units.

which are often dysregulated in malignant cells. ABT-737, which is a BH3 mimetic, could inhibit Bcl-xL, Bcl-2, and Bcl-w, and it has induced the regression of solid tumors (23). We previously reported that high dose ABT-737 administration caused hepatocyte apoptosis even in a normal liver, which was partly due to constitutive Bid-mediated BH3 stress (7). This finding led us to investigate the involvement of Bim and Bid in this ABT-737-mediated hepatotoxicity. Bim/Bid double knock-out mice (*bim*$^{-/-}$*bid*$^{-/-}$) were generated by mating Bim knock-out mice (*bim*$^{-/-}$) with Bid knock-out mice (*bid*$^{-/-}$), and the offspring were then treated with this drug. Western blot analysis confirmed the efficient deletion of Bim and Bid from the liver tissue of the double knock-out mice (Fig. 5*A*). Upon ABT-737 treatment, the Bim/Bid double knock-out mice showed complete prevention of ABT-737-induced hepatocyte apoptosis and hepatotoxicity (Fig. 5, *B–F*), in sharp con-

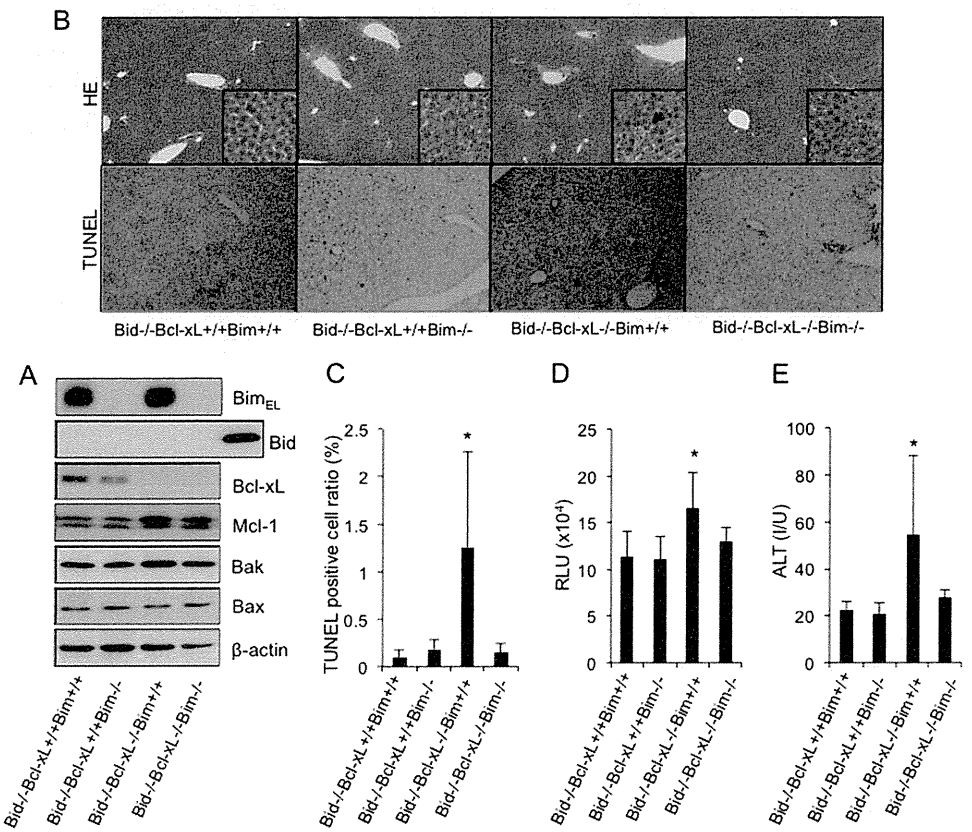

FIGURE 3. **The disruption of Bim and Bid prevented spontaneous hepatocyte apoptosis in the absence of Bcl-xL.** The offspring from the mating of *bim*$^{+/-}$*bid*$^{-/-}$*bcl-x*$^{flox/flox}$*alb-cre* mice with *bim*$^{+/-}$*bid*$^{-/-}$*bcl-x*$^{flox/flox}$ mice were examined at 6 weeks of age. *Bcl-xL*$^{+/+}$ and *Bcl-xL*$^{-/-}$, *bcl-x*$^{flox/flox}$ and *bcl-x*$^{flox/flox}$*alb-cre*, respectively. *A*, Western blot analysis of whole liver lysates for the expression of Bim$_{EL}$, Bid, Bcl-xL, Mcl-1, Bak, Bax, and β-actin. *B*, representative images of liver histology stained with hematoxylin-eosin (*HE*) and TUNEL (original magnifications, ×100 (*large panels*) and ×400 (*insets*)). *Black arrows* indicate apoptotic bodies. *C*, TUNEL-positive cell ratio; more than 5 mice/group; *, $p < 0.05$ *versus* all. *D*, serum caspase-3/7 activity; more than 6 mice/group; *, $p < 0.05$ *versus* all. *E*, serum ALT levels; more than 6 mice/group; *, $p < 0.05$ *versus* all. *Error bars*, S.D. *RLU*, relative light units; *I/U*, international units.

trast to their Bid-knock-out littermates, which still showed moderate hepatocyte apoptosis (Fig. 5, *C–E*) and increased serum ALT levels (Fig. 5*F*). These findings suggested that Bim- and Bid-mediated constant BH3 stress evoked hepatotoxicity by promoting the intrinsic pathway of apoptosis with the use of the inhibitors of the Bcl-2 family.

DISCUSSION

At least eight BH3-only proteins are known, and five have been reported to exist in hepatocytes: Bid, Bim, Noxa, Puma, and Bad (22). We also confirmed these five proteins in the liver tissue of our mice (Fig. 1*A*), and we detected at least the mRNA expression of three other genes (supplemental Fig. 1). These proteins are considered to function as pro-apoptotic sensors upon activation by a variety of apoptotic stimuli, thereby promoting an intrinsic pathway of apoptosis in a manner that is dependent on the presence of Bak and Bax. In previous studies, bile acids or death receptor stimuli activated Bid and induced liver injury, which was alleviated by Bid disruption (12, 22). Bim activation was involved in hepatocyte lipoapoptosis, which is a critical feature of non-alcoholic steatohepatitis, and in reactive oxygen species-induced hepatocyte apoptosis (10, 11, 14). Additionally, a recent *in vivo* study revealed that the activation of Bid and Bim played a central pro-apoptotic role in fatal TNF-α-induced hepatitis (24). Taken together, these findings indicated the importance of these two BH3-only proteins in the pathogenesis of various liver diseases (12, 24, 25). Conversely, the systemic knock-out of Bid or Bim in mice did not result in any liver abnormalities under normal conditions; therefore, there has not been much interest in studying their physiological involvement in the healthy liver (12, 26). However, our present study showed that spontaneous hepatocyte apoptosis in the absence of Bcl-xL was alleviated by the deletion of either Bim or Bid, and it was diminished by the deletion of both. These results indicated that these BH3-only proteins are functionally active even in the healthy liver, but they are fully restrained by the anti-apoptotic Bcl-2 family proteins in the physiological state.

What type of stimuli constitutively activate these BH3-only proteins remains unknown. The liver is a specific organ that can be continuously exposed to a variety of stimuli, such as bile acids and enteric endotoxin, as well as interactions with immune cells. These stimuli might cause constitutive BH3-only stress through the activation of death receptors, such as Fas, tumor necrosis factor (TNF), and TNF-related apoptosis-inducing ligand (TRAIL) receptors. To explore the involvement of Fas signaling in generating this BH3-only stress, we studied the effect of *fas* inhibition in the hepatocyte apoptosis induced by the genetic disruption of Bcl-xL or ABT-737 administration. siRNA-mediated *in vivo* knockdown of *fas* did not alleviate their hepatocyte apoptosis (supplemental Fig. 2, *B* and *D*), suggesting that Fas signaling may not be the origin of this BH3-only

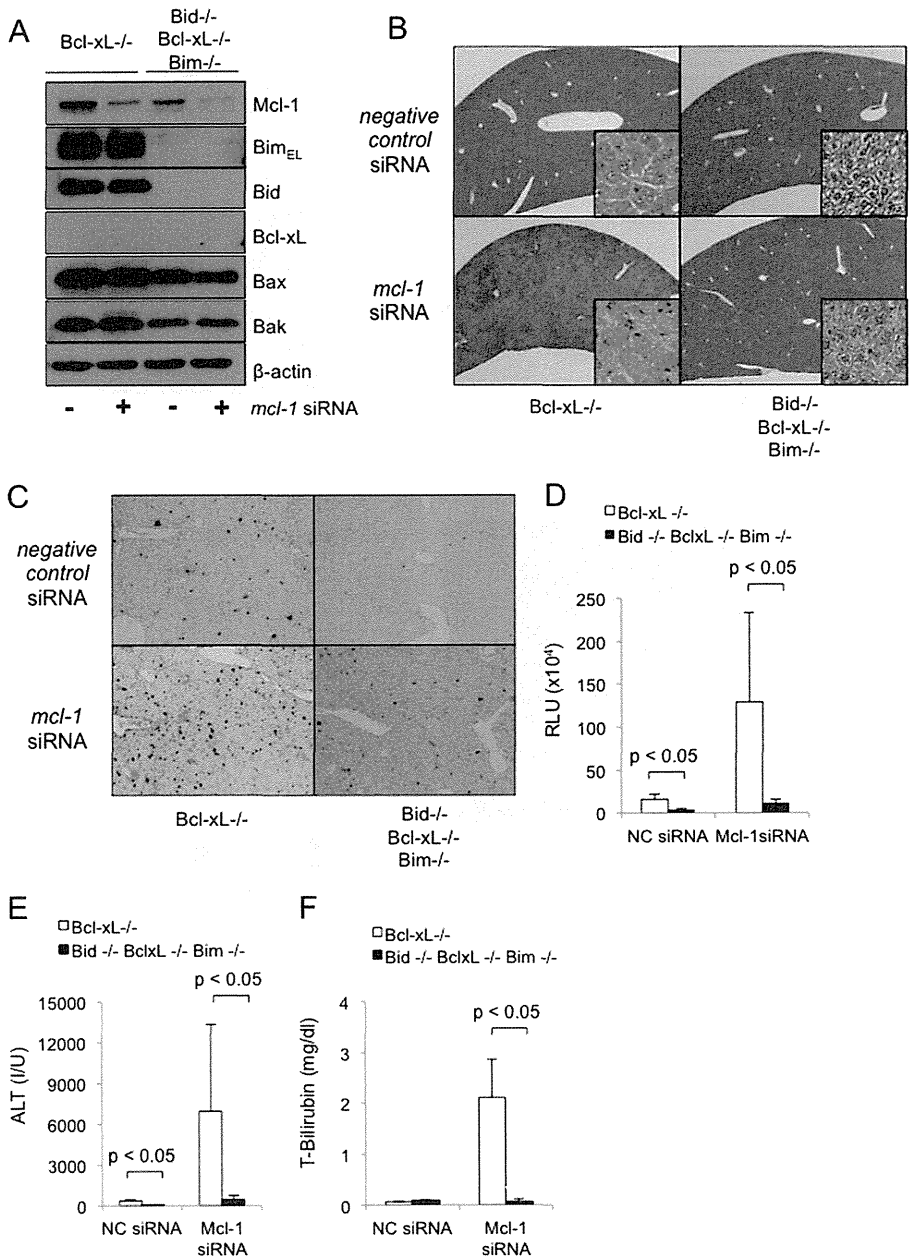

FIGURE 4. **Bim and Bid are essential regulators involved in the intrinsic pathway of apoptosis in hepatocytes in the absence of anti-apoptotic Bcl-2 family proteins.** *bcl-x$^{flox/flox}$alb-cre* mice and *bim$^{-/-}$bid$^{-/-}$bcl-x$^{flox/flox}$alb-cre* mice were injected with *mcl-1* or with negative control siRNA via the tail vein and were sacrificed 24 h (*A* and *C–F*) or 48 h (*B*) later. *Bcl-xL$^{+/+}$* and *Bcl-xL$^{-/-}$*, *bcl-x$^{flox/flox}$* and *bcl-x$^{flox/flox}$alb-cre*, respectively. *NC*, negative control. *A*, Western blot analysis of whole liver lysates for the expression of Bim$_{EL}$, Bid, Bcl-xL, Mcl-1, Bak, Bax, and β-actin. *B*, representative images of liver histology stained with hematoxylin-eosin (original magnifications, ×100 (*large panels*) and ×400 (*insets*)). *C*, representative images of liver histology stained with TUNEL (original magnification, ×100). *D*, serum caspase-3/7 activity; $n = 3–4$ mice/group. *E*, serum ALT levels; $n = 4$ mice/group; data are presented as means ± S.E. (*error bars*). *F*, serum T-bilirubin levels; $n = 4$ mice/group. *RLU*, relative light units; *I/U*, international units.

stress. However, it should be noted here that siRNA administration only decreased *fas* mRNA levels to around half (supplemental Fig. 2, *A* and *C*). Therefore, genetic study is still necessary to clarify its involvement. In order to examine the involvement of T and B cells, which comprise about 50% of intrahepatic resident immune cells (27), in producing the BH3-only stress in the healthy liver, we crossed hepatocyte-specific Mcl-1 knock-out mice with homozygous SCID mutant mice, which are characterized by an absence of functional T cells and B cells (28). The spontaneous hepatocyte apoptosis of the Mcl-1 knock-out mice was unchanged even in the homozygous SCID mutant background, monitored by serum ALT levels and serum caspase-3/7 activity (supplemental Fig. 3, *A–D*). These data indicate that these immune cells are not the major source of the BH3-only stress in the liver under physiological conditions. Therefore, further study is required to identify the main source of constitutive BH3-only stress in the healthy liver. We previously reported that Mcl-1 and Bcl-xL individually worked as apoptotic antagonists in differentiated hepatocytes (13). However, the hepatocyte-specific deletion of both led to early postnatal death due to the failure of hepatocyte development in the fetal liver (13), thus hampering the clarification of their

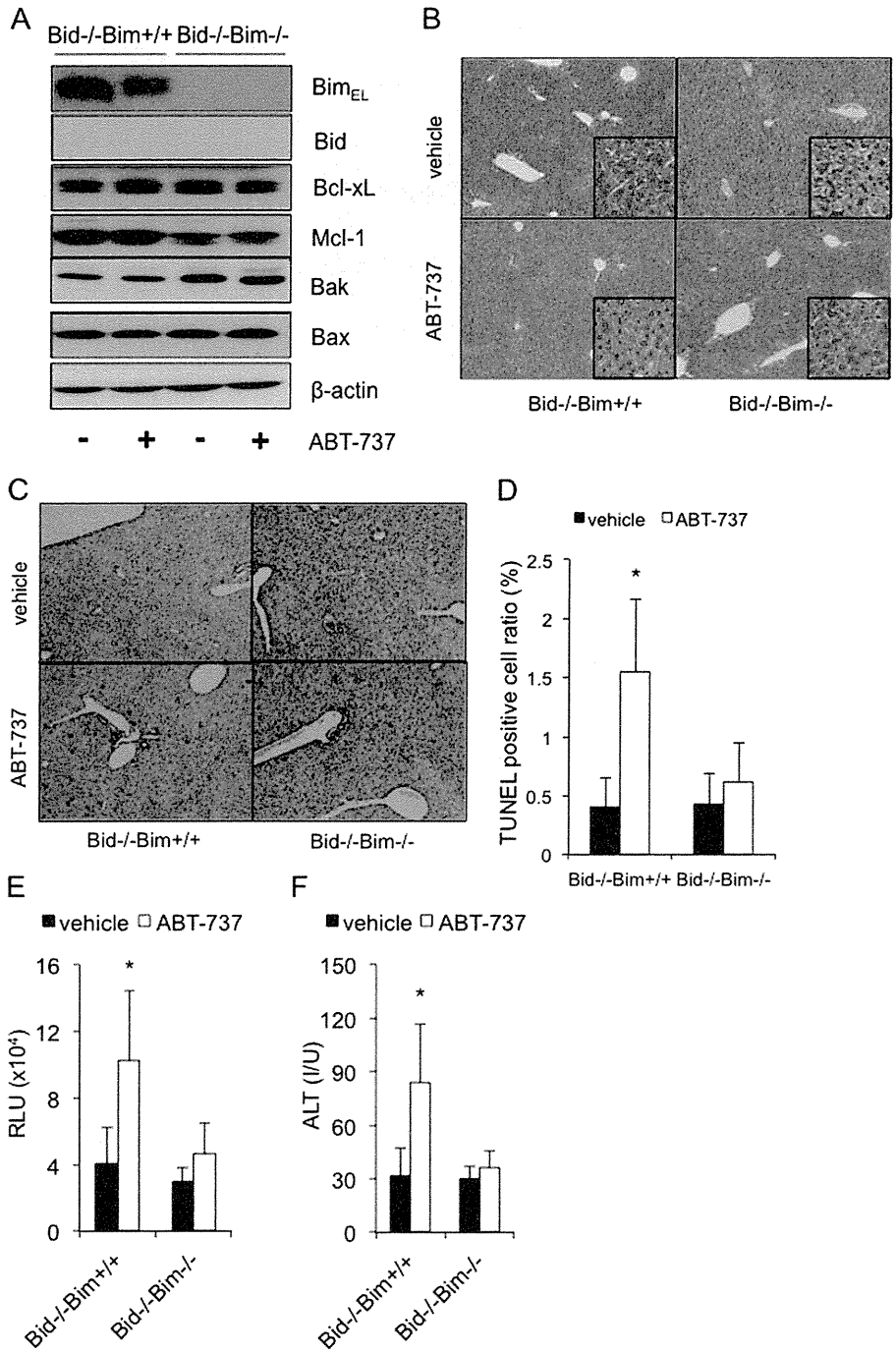

FIGURE 5. **The presence of Bim- and Bid-induced constant BH3 stress in the healthy liver causes hepatotoxicity with the use of anti-cancer agents that target anti-apoptotic Bcl-2 family proteins.** The offspring from *bim*$^{+/-}$*bid*$^{-/-}$ mating pairs were given an intraperitoneal injection of ABT-737 (100 mg/kg) or vehicle and were examined after 6 h. *A*, Western blot analysis of whole liver lysates for the expression of Bim$_{EL}$, Bid, Bcl-xL, Mcl-1, Bak, Bax, and β-actin. *B* and *C*, representative images of liver histology stained with hematoxylin-eosin and TUNEL (original magnifications, ×100 (*large panels*) and ×400 (*insets*)). *D*, TUNEL-positive cell ratio; $n = 5$–6 mice/group; *, $p < 0.05$ *versus* all. *E*, serum caspase-3/7 activity; more than 5 mice/group; *, $p < 0.05$ *versus* all. *F*, serum ALT levels; more than 5 mice/group; *, $p < 0.05$ *versus* all. *Error bars*, S.D. *RLU*, relative light units; *I/U*, international units.

cooperative involvement in the adult liver. In the present study, the combination of genetically engineered mice and *in vivo* siRNA technology enabled the investigation of their cooperative roles for the first time, and we found that the inhibition of Mcl-1 caused sublethal liver injury with massive hepatocyte apoptosis in Bcl-xL-knock-out mice. Meanwhile, we also found that sublethal apoptosis was prevented in a Bim/Bid double knock-out background, suggesting that, of the BH3-only proteins, Bim and Bid are important for activating the intrinsic pathway of hepatocyte apoptosis in the absence of anti-apoptotic Bcl-2 family proteins. It would also be interesting to determine whether other anti-apoptotic Bcl-2 family proteins or BH3-only proteins are involved in this healthy Bcl-2 rheostasis.

The anti-apoptotic Bcl-2 family proteins are often dysregulated in a variety of malignancies, and they have been recog-

nized as important oncogenes (29). ABT-737, which was recently developed to inhibit the Bcl-xL, Bcl-w, and Bcl-2 proteins, displays anti-tumor activity against lymphoid malignancies and small-cell lung carcinoma (23). These drugs were considered to selectively target tumor cells because malignant cells receive many genotoxic and environmental stress-induced BH3-only signals, so these cells are thus dependent on the anti-apoptotic Bcl-2 family members for their survival. However, we previously reported that the high-dose administration of ABT-737 (100 mg/kg) elicited hepatotoxicity via Bak/Bax-dependent apoptosis in normal hepatocytes (7), suggesting that dependence on the anti-apoptotic Bcl-2 family proteins is not a specific feature of tumor cells but is the case in healthy liver cells. In the present study, we demonstrated that the disruption of Bim and Bid completely prevented hepatocyte apoptosis and hepatotoxicity induced by high dose ABT-737 (100 mg/kg), suggesting that these proteins are responsible for this hepatotoxicity. Meanwhile, although 25 mg/kg ABT-737, which is relatively close to the clinical dose, caused moderate hepatocyte apoptosis, this apoptosis was completely blocked by Bid inhibition (supplemental Fig. 4). Therefore, it is unclear whether both Bid and Bim are truly involved in hepatotoxicity when using ABT-737 at clinically relevant doses.

This study demonstrated that Bim was also involved in the hepatocyte apoptosis caused by Mcl-1 deficiency in addition to Bid, which was noted in our previous report (13). Several previous human studies have reported that Mcl-1 proteins were down-regulated in the liver tissues of non-alcoholic steatohepatitis and primary biliary cirrhosis patients (30, 31), and experimental studies have demonstrated that Mcl-1 down-regulation by saturated fatty acids caused hepatocyte lipoapoptosis, which plays an important role in the development of fatty liver disease (32, 33). Taken together with our findings, these reports suggest the possibility that Bim- and Bid-mediated constant BH3 stresses might constitute therapeutic targets of the hepatotoxicity observed in these human liver diseases.

In conclusion, we have demonstrated that the novel rheostatic balance between the pro-apoptotic BH3-only proteins Bim and Bid and the anti-apoptotic Bcl-2 family proteins Bcl-xL and Mcl-1 regulates hepatocyte life and death in the physiological state. Our present study sheds new light on the dynamic and well orchestrated Bcl-2 networks in the healthy liver.

Acknowledgments—We thank Lothar Hennighausen (National Institutes of Health) and Dr. You-Wen He (Duke University) for providing the floxed bcl-x mice and floxed mcl-1 mice, respectively. We also thank Abbott Laboratories for providing ABT-737.

REFERENCES

1. Youle, R. J., and Strasser, A. (2008) The BCL-2 protein family. Opposing activities that mediate cell death. *Nat. Rev. Mol. Cell Biol.* **9,** 47–59
2. Chipuk, J. E., and Green, D. R. (2008) How do BCL-2 proteins induce mitochondrial outer membrane permeabilization? *Trends Cell Biol.* **18,** 157–164
3. Adams, J. M., and Cory, S. (2007) Bcl-2-regulated apoptosis. Mechanism and therapeutic potential. *Curr. Opin. Immunol.* **19,** 488–496
4. Kim, H., Rafiuddin-Shah, M., Tu, H. C., Jeffers, J. R., Zambetti, G. P., Hsieh, J. J., and Cheng, E. H. (2006) Hierarchical regulation of mitochondrion-dependent apoptosis by BCL-2 subfamilies. *Nat. Cell Biol.* **8,** 1348–1358
5. Willis, S. N., Fletcher, J. I., Kaufmann, T., van Delft, M. F., Chen, L., Czabotar, P. E., Ierino, H., Lee, E. F., Fairlie, W. D., Bouillet, P., Strasser, A., Kluck, R. M., Adams, J. M., and Huang, D. C. (2007) Apoptosis initiated when BH3 ligands engage multiple Bcl-2 homologs, not Bax or Bak. *Science* **315,** 856–859
6. Korsmeyer, S. J., Shutter, J. R., Veis, D. J., Merry, D. E., and Oltvai, Z. N. (1993) Bcl-2/Bax. A rheostat that regulates an anti-oxidant pathway and cell death. *Semin. Cancer Biol.* **4,** 327–332
7. Hikita, H., Takehara, T., Kodama, T., Shimizu, S., Hosui, A., Miyagi, T., Tatsumi, T., Ishida, H., Ohkawa, K., Li, W., Kanto, T., Hiramatsu, N., Hennighausen, L., Yin, X. M., and Hayashi, N. (2009) BH3-only protein bid participates in the Bcl-2 network in healthy liver cells. *Hepatology* **50,** 1972–1980
8. Giam, M., Huang, D. C., and Bouillet, P. (2008) BH3-only proteins and their roles in programmed cell death. *Oncogene* **27,** Suppl. 1, S128–S136
9. Lomonosova, E., and Chinnadurai, G. (2008) *Oncogene* **27,** Suppl. 1, S2–S19
10. Barreyro, F. J., Kobayashi, S., Bronk, S. F., Werneburg, N. W., Malhi, H., and Gores, G. J. (2007) Transcriptional regulation of Bim by FoxO3A mediates hepatocyte lipoapoptosis. *J. Biol. Chem.* **282,** 27141–27154
11. Ishihara, Y., Takeuchi, K., Ito, F., and Shimamoto, N. (2011) Dual regulation of hepatocyte apoptosis by reactive oxygen species. Increases in transcriptional expression and decreases in proteasomal degradation of BimEL. *J. Cell Physiol.* **226,** 1007–1016
12. Yin, X. M., Wang, K., Gross, A., Zhao, Y., Zinkel, S., Klocke, B., Roth, K. A., and Korsmeyer, S. J. (1999) Bid-deficient mice are resistant to Fas-induced hepatocellular apoptosis. *Nature* **400,** 886–891
13. Hikita, H., Takehara, T., Shimizu, S., Kodama, T., Li, W., Miyagi, T., Hosui, A., Ishida, H., Ohkawa, K., Kanto, T., Hiramatsu, N., Yin, X. M., Hennighausen, L., Tatsumi, T., and Hayashi, N. (2009) Mcl-1 and Bcl-xL cooperatively maintain integrity of hepatocytes in developing and adult murine liver. *Hepatology* **50,** 1217–1226
14. Ishihara, Y., Ito, F., and Shimamoto, N. (2011) Increased expression of c-Fos by extracellular signal-regulated kinase activation under sustained oxidative stress elicits BimEL upregulation and hepatocyte apoptosis. *FEBS J.* **278,** 1873–1881
15. Malhi, H., Bronk, S. F., Werneburg, N. W., and Gores, G. J. (2006) Free fatty acids induce JNK-dependent hepatocyte lipoapoptosis. *J. Biol. Chem.* **281,** 12093–12101
16. Dzhagalov, I., St John, A., and He, Y. W. (2007) The antiapoptotic protein Mcl-1 is essential for the survival of neutrophils but not macrophages. *Blood* **109,** 1620–1626
17. Takehara, T., Tatsumi, T., Suzuki, T., Rucker, E. B., 3rd, Hennighausen, L., Jinushi, M., Miyagi, T., Kanazawa, Y., and Hayashi, N. (2004) Hepatocyte-specific disruption of Bcl-xL leads to continuous hepatocyte apoptosis and liver fibrotic responses. *Gastroenterology* **127,** 1189–1197
18. Wagner, K. U., Claudio, E., Rucker, E. B., 3rd, Riedlinger, G., Broussard, C., Schwartzberg, P. L., Siebenlist, U., and Hennighausen, L. (2000) Conditional deletion of the Bcl-x gene from erythroid cells results in hemolytic anemia and profound splenomegaly. *Development* **127,** 4949–4958
19. Maruyama, C., Suemizu, H., Tamamushi, S., Kimoto, S., Tamaoki, N., and Ohnishi, Y. (2002) Genotyping the mouse severe combined immunodeficiency mutation using the polymerase chain reaction with confronting two-pair primers (PCR-CTPP). *Exp. Anim.* **51,** 391–393
20. Kodama, T., Takehara, T., Hikita, H., Shimizu, S., Shigekawa, M., Tsunematsu, H., Li, W., Miyagi, T., Hosui, A., Tatsumi, T., Ishida, H., Kanto, T., Hiramatsu, N., Kubota, S., Takigawa, M., Tomimaru, Y., Tomokuni, A., Nagano, H., Doki, Y., Mori, M., and Hayashi, N. (2011) Increases in p53 expression induce CTGF synthesis by mouse and human hepatocytes and result in liver fibrosis in mice. *J. Clin. Invest.* **121,** 3343–3356
21. Kodama, T., Takehara, T., Hikita, H., Shimizu, S., Li, W., Miyagi, T., Hosui, A., Tatsumi, T., Ishida, H., Tadokoro, S., Ido, A., Tsubouchi, H., and Hayashi, N. (2010) Thrombocytopenia exacerbates cholestasis-induced liver fibrosis in mice. *Gastroenterology* **138,** 2487–2498, 2498.e2481–2487
22. Baskin-Bey, E. S., and Gores, G. J. (2005) Death by association. BH3 domain-only proteins and liver injury. *Am. J. Physiol. Gastrointest. Liver Physiol.* **289,** G987–G990
23. Oltersdorf, T., Elmore, S. W., Shoemaker, A. R., Armstrong, R. C., Augeri,